TROPICAL CYCLONE RESEARCH REPORT
TCRR (2016) **No 1**: 1–24
Meteorological Institute
Ludwig Maximilians University of Munich

Recent Developments in the Fluid Dynamics of Tropical Cyclones

Michael T. Montgomery[a] [1] and Roger K. Smith[b]
[a] *Dept. of Meteorology, Naval Postgraduate School, Monterey, CA.*
[b] *Meteorological Institute, Ludwig Maximilians University of Munich, Munich, Germany*

Abstract: This paper reviews progress in understanding the fluid dynamics and moist thermodynamics of tropical cyclone vortices. The focus is on the dynamics and moist thermodynamics of vortex intensification and structure and the role of coherent eddy structures in the evolution of these vortices. We have sought to give an appraisal of previous ideas on many facets of the subject and have articulated also some open questions. The advances reviewed herein provide new insight and tools for interpreting complex vortex-convective phenomenology in simulated and observed tropical cyclones.

KEY WORDS Tropical cyclone intensification, rotating deep convection, boundary layer control, size-growth, potential intensity, quasi steady-state hurricanes

Date: April 12, 2016

1 Introduction

Tropical cyclones are fascinating large-scale, organized, convective vortices that continue to hold many scientific secrets regarding their birth, intensification, mature evolution and decay. These moist convective vortices comprise arguably all facets of classical fluid dynamics ranging from the microscale flow in and around small droplets, the coalescence of smaller droplets into larger ones, precipitation and evaporation processes, to the larger scales of buoyant thermals in a rotating environment, their aggregate effects on the vortex circulation, and to the even larger scale of vortex waves and eddies, such as inertia-buoyancy waves, vortex Rossby waves, eyewall mesovortices and their interaction with the vortex circulation. The large Reynolds numbers of these flows implies that turbulence of the Kolmogorov kind will be an element at the small scales, but the presence of strong, spatially variable, vertical rotation in these systems suggests that quasi-two dimensional fluid dynamics and its associated turbulence phenomenology should be an important element also with modifications due to the presence of deep moist convection, which is intrinsically three-dimensional. The more intense manifestations of these vortices (maximum near-surface wind speed > 32 m s^{-1}) are called hurricanes in the Atlantic and Eastern Pacific basins and typhoons in the Western North Pacific region.

Although flow speeds are well below the sound speed (typically < 100 m s^{-1}), non-conservative effects, principally associated with friction at the ocean surface and wind-forced transfer of moisture and heat from the warm sea, make tropical cyclones a particularly interesting and challenging scientific problem to understand. Practical considerations, such as saving human life and property in the path of these storms are another important driving factor in the quest for knowledge about them. Atlantic Hurricane Sandy (2012) is a reminder that even tropical storms (maximum near-surface wind speed < 32 m s^{-1}) can wreak havoc on populated coastal communities, maritime assets and even inland populations (e.g. Lussier et al. 2015). As coastal communities continue to grow in tropical cyclone affected regions, there is an increasing demand for more accurate tropical cyclone forecasts.

There are two main aspects of the forecasting problem. The first is to forecast the storm track, and the second is to forecast its intensity, characterized typically by the maximum near-surface wind speed. Track forecasts have improved significantly in the past 25 years, but progress in intensity forecasting has shown comparatively little improvement (DeMaria et al. 2005; Rogers and Coauthors 2006). Because the track depends mainly on the large-scale flow in which the vortex is embedded, the improvement in track forecasting may be attributed largely to the improvement in the representation of the large-scale flow around the vortex by global forecast models. In contrast, the intensity appears to depend on processes of wide ranging scales spanning many orders of magnitude as noted above.

Because of the challenges of forecasting tropical cyclone intensity change, the problem of understanding how intensity change occurs has been at the forefront of tropical cyclone research in recent years, especially in the context of the rapid intensification or decay of storms. These challenges are motivated by the recent instigation of the Hurricane Forecast Improvement Project (HFIP) by the National Oceanic and Atmospheric Administration

[1] Correspondence to: Michael T. Montgomery, Naval Postgraduate School, 159 Dyer Rd., Root Hall, Monterey, CA 93943. E-mail: mtmontgo@nps.edu

(NOAA) and other U. S. Government agencies to coordinate hurricane research necessary to accelerate improvements in hurricane track and intensity forecasts (Gall et al. 2013).

There have been significant advances in understanding tropical cyclone behaviour since the earlier reviews of the topic by Emanuel (1991) and Chan (2005) and the field has broadened significantly. As a result, a comprehensive review of all fluid dynamical aspects is not possible in the space available to us. For this reason we have chosen to focus on the dynamics and thermodynamics of the vortex when viewed as a coherent structure with embedded substructures. To begin, for those readers working in other fields, we review briefly in section 2 the equations of motion and some other basic concepts involving zero-order force balances, moist thermodynamics and deep convective clouds in a rotating environment. This material provides a reference for much of the later discussion. Some readers may wish to skip this section.

In section 3 we survey progress that has been made in understanding tropical cyclone intensification and structure from the perspective of the prototype intensification problem, which considers for simplicity the spin up of an initially balanced, axisymmetric, cloud-free, conditionally-unstable, baroclinic vortex of near tropical storm strength in a quiescent tropical environment on an f-plane. Here, paradigms for vortex intensification including emerging ideas pointing to the importance of boundary layer control in vortex evolution are discussed. In sections 4 we examine more deeply the role of cloud-generated vorticity in supporting vortex spin up. Progress in understanding mature vortex intensity is reviewed in section 5 and the steady-state problem is reviewed in section 6. The conclusions are given in section 7.

Because of space constraints, we are unable review aspects of vortex motion, vortex Rossby waves and their contribution to vortex resilience, nor the early stages of storm formation. For the same reason we cannot address topics such as: the interaction of storms with ambient vertical shear; helicity; secondary eyewall formation; ocean feedback effects; the interaction with neighbouring weather systems including fronts and upper troughs; the extratropical transition when storms move into the middle latitudes; cloud microphysics; boundary layer rolls; wind wave coupling; and details of the surface layer (or emulsion layer).

2 Preliminaries

To provide a common framework for this review, we present the equations of motion pertinent to understanding tropical cyclone behaviour.

2.1 The equations in cylindrical polar coordinates

Because an intensifying tropical cyclone exhibits some degree of circular organization (though not axially symmetric), it is advantageous to express the equations of motion in cylindrical polar coordinates, (r, λ, z). The rotation of the Earth is incorporated by the addition of Coriolis and centrifugal forces in the usual manner (Gill 1982; Holton 2004) and, because of the relatively limited horizontal scale of the tropical cyclone circulation, the rotation rate is assumed to be independent of latitude (i.e., a so-called f-plane, where f is the Coriolis parameter given by $f = 2\Omega \sin\phi$, Ω is the Earth's rotation rate, and ϕ is latitude). The governing equations are:

$$\frac{\partial u}{\partial t} + u\frac{\partial u}{\partial r} + \frac{v}{r}\frac{\partial u}{\partial \lambda} + w\frac{\partial u}{\partial z} - \frac{v^2}{r} - fv = -\frac{1}{\rho}\frac{\partial p}{\partial r} + F_r, \tag{1}$$

$$\frac{\partial v}{\partial t} + u\frac{\partial v}{\partial r} + \frac{v}{r}\frac{\partial v}{\partial \lambda} + w\frac{\partial v}{\partial z} + \frac{uv}{r} + fu = -\frac{1}{\rho r}\frac{\partial p}{\partial \lambda} + F_\lambda, \tag{2}$$

$$\frac{\partial w}{\partial t} + u\frac{\partial w}{\partial r} + \frac{v}{r}\frac{\partial w}{\partial \lambda} + w\frac{\partial w}{\partial z} = -\frac{1}{\rho}\frac{\partial p}{\partial z} - g + F_z, \tag{3}$$

$$\frac{\partial \rho}{\partial t} + \frac{1}{r}\frac{\partial \rho r u}{\partial r} + \frac{1}{r}\frac{\partial \rho v}{\partial \lambda} + \frac{\partial \rho w}{\partial z} = 0, \tag{4}$$

$$\frac{\partial \theta}{\partial t} + u\frac{\partial \theta}{\partial r} + \frac{v}{r}\frac{\partial \theta}{\partial \lambda} + w\frac{\partial \theta}{\partial z} = \dot{\theta} + F_\theta, \tag{5}$$

$$\rho = p_* \pi^{\frac{1}{\kappa}-1}/(R\theta) \tag{6}$$

where u, v, w are the velocity components in the three coordinate directions, θ is the potential temperature, $\dot{\theta}$ is the diabatic heating rate $(1/c_p\pi)Dh/Dt$, h is the heating rate per unit mass expressed as J kg^{-1} s^{-1}, $\pi = (p/p_*)^\kappa$ is the Exner function, p the pressure, g the effective gravitational force per unit mass, R the specific gas constant for dry air, c_p the specific heat at constant pressure, $\kappa = R/c_p$ and $p_* = 1000$ mb is a reference pressure. The temperature is given by $T = \pi\theta$. The terms (F_r, F_λ, F_z) represent unresolved processes associated with turbulent momentum diffusion. In the case of numerical models, these terms specifically represent a divergence of sub-grid scale eddy momentum flux associated with unresolved processes such as convection for a model that cannot resolve clouds and/or frictional stress at the lower surface and related mixing processes in the frictional boundary layer. Similarly, F_θ represents the effects of turbulent heat transport (again possibly including those associated with convection for a coarse resolution model). The foregoing equations comprise the three components of the momentum equation, the continuity equation, the thermodynamic equation and the ideal gas equation of state, respectively. In the foregoing equations, the traditional approximation is made of neglecting the horizontal component of the earth's rotation rate and other metric terms associated with the approximate sphericity of the Earth that are small on account of the limited horizontal scale of a typical hurricane vortex compared to the mean radius of the Earth. In the above equation set, it is assumed that the origin of coordinates is located at some suitably defined vortex centre.

In moist flows, the equations need to be supplemented by tendency equations for the water vapour mixing ratio,

q_v, and of various species of water substance, while θ in the equation of state must be replaced by the virtual potential temperature, θ_v.

2.2 Solution for a freely-spinning vortex

For adiabatic frictionless flow [$\dot{\theta} = 0$, $(F_r, F_\lambda, F_z) = (0, 0, 0)$], Eqs. (1) - (5) have a solution, $v(r, z)$, for a steady freely spinning vortex in which u and w are identically zero and $v(r, z)$ is an arbitrary function of r and z. Such a vortex is in *gradient wind balance* $[(1/\rho)(\partial p/\partial r) = C]$ and *hydrostatic balance* $[-(1/\rho)(\partial p/\partial z) = -g]$, where $C = v^2/r + fv$ is the sum of the specific centrifugal and Coriolis forces. The ratio of centrifugal to Coriolis forces is a vortex Rossby number, $Ro = v/fr$. Near the radius of maximum tangential wind Ro is of order unity for a tropical depression strength vortex and can be as large as several hundred for a mature hurricane or typhoon.

Multiplying the gradient wind and hydrostatic balance equations by ρ and cross-differentiating to eliminate the pressure leads to the thermal wind equation

$$\frac{\partial \log \rho}{\partial r} + \frac{C}{g}\frac{\partial \log \rho}{\partial z} = -\frac{1}{g}\frac{\partial C}{\partial z}. \tag{7}$$

This first-order linear partial differential equation relates the logarithm of density $\log \rho(r, z)$ (or equivalently $\log \theta$) to the vertical gradient of C and hence the vertical shear of the swirling wind. The characteristics of the equation satisfy $dz/dr = C/g$ and are just the isobaric surfaces. For further details, see Smith (2006, 2007).

2.3 Zero order force balances and the agradient force

A scale analysis of the equations of motion for a tropical cyclone vortex having a characteristic height-to-width aspect ratio squared $(H/L)^2$ much less than unity shows that except near the surface and in the upper troposphere, the primary (tangential) circulation of a mature hurricane is approximately axisymmetric and in gradient wind and hydrostatic balance (i.e. the underlined terms in Eqs. (1) and (3)). Accordingly, the freely-spinning vortex solution of section 2.2 represents a meaningful zero order approximation for the bulk vortex. It is then useful to enquire about the imbalance of forces in the meridional (r, z) plane, the so-called *agradient force*, $\mathbf{F_a}$. Defining density and pressure perturbations, ρ' and p', relative to the corresponding quantities in the dynamically balanced state as defined above, $\rho_R(r, z)$ and $p_R(r, z)$, the inviscid form of Eqs. (1) and (3) may be written in vector form:

$$\frac{D\mathbf{u}}{Dt} = \mathbf{F_a}, \tag{8}$$

where

$$\mathbf{F_a} = -\frac{1}{\rho}\nabla p' + \mathbf{g}\frac{\rho'}{\rho}, \tag{9}$$

$\mathbf{u}$ is the transverse velocity vector (u, w), and $\mathbf{g} = (C, 0, -g)$ is the *generalized gravitational vector*. The vector quantity on the right-hand-side of (9) is the *agradient force* and the term $\mathbf{g}\rho'/\rho$ is the *generalized buoyancy force*. Equation (9) shows that lighter air parcels than the local density associated with the balanced vortex (i.e., $\rho' < 0$) are positively buoyant in the vertical and have an inward component of generalized buoyancy (Smith et al. 2005). Although the radial component of the generalized gravitational vector is small compared to the vertical component in tropical cyclone vortices, the effect of the radial component of the generalized buoyancy force by itself is to move buoyant plumes inwards. In actual fact, however, the inner-core clouds tilt outwards so that the radial component of $\mathbf{F_a}$ must be dominated by the perturbation pressure gradient, which is generally directed outwards.

2.4 Absolute angular momentum and centrifugal stability

Multiplication of Eq. (2) by r and a little manipulation leads to the equation

$$\frac{\partial M}{\partial t} + u\frac{\partial M}{\partial r} + \frac{v}{r}\frac{\partial M}{\partial \lambda} + w\frac{\partial M}{\partial z} = -\frac{1}{\rho}\frac{\partial p}{\partial \lambda} + rF_\lambda, \tag{10}$$

where $M = rv + \frac{1}{2}fr^2$ is the *absolute angular momentum per unit mass* of an air parcel about the rotation axis. For axisymmetric $(\partial/\partial\lambda = 0)$ and frictionless $(F_\lambda = 0)$ flow, the right-hand-side of (10) is zero and M is materially conserved as rings of air move radially and vertically.

The freely-spinning vortex solution of section 2.2 is stable to small, axisymmetric radial displacements if the local *inertial (centrifugal) stability parameter*, $I^2 = (1/r^3)\partial M^2/\partial r$, is positive. The quantity I^2 is a measure of the inertial stiffness of the vortex and is analogous to the *static stability parameter*, $N^2 = (g/\theta)(d\theta/dz)$, which is a measure of the resistance to vertical displacements in a stably stratified fluid (Holton 2004, p 54). Tropical cyclones generally have M-distributions that increase monotonically with radius in the bulk of the troposphere (e.g. Franklin et al. 1993) and are therefore centrifugally stable. Even if stable to radial and vertical displacements, the vortex may be unstable to displacements in other directions, a condition known as symmetric instability (e.g. Shapiro and Montgomery 1993).

2.5 Moist deep convection

Significant weather over the tropical oceans is generally associated with thunderstorms or clusters of thunderstorms that may be part of larger scale circulations. Tropical cyclones are the end stage of a few of these storm clusters. Thunderstorms are manifestations of deep moist convection, which from a fluid dynamical perspective has properties that differ in important ways from those of dry convection (Emanuel 1994). An understanding of the dynamics of tropical cyclones rests to a considerable extent on an understanding of deep convection, which for space reasons

cannot covered here. For in-depth discussions of moist convection, the reader is referred to texts by Emanuel (1994) and Houze (2014).

2.6 Rotating deep convection

When buoyant convection occurs in an environment with non-zero vertical vorticity, the convective updraughts amplify the vorticity by the process of vortex-tube stretching (e.g., Julien et al. 1996; Hendricks et al. 2004; Wissmeier and Smith 2011; Kilroy and Smith 2013). Typically, the vorticity may be amplified by between 1 and 2 orders of magnitude on the scale of the cloud updraughts. While the updraught strengths are generally much weaker than in mid-latitude supercell thunderstorms, as are the associated local tangential wind components (see e.g. Klemp 1987; Rotunno 2013), the presence of these vortical cores would appear to be important in the genesis and intensification of tropical cyclones.

The role of rotating deep convective clouds and their aggregation in the amplification of the larger-scale vortex has been the subject of recent numerical and theoretical investigations (Hendricks et al. 2004; Montgomery et al. 2006b; Nguyen et al. 2008; Shin and Smith 2014; Fang and Zhang 2011; Braun et al. 2010; Gopalakrishnan et al. 2011; Schecter 2011), but questions remain about the quantitative importance of the enhanced vorticity within the clouds themselves. We explore these issues further in section 4.

2.7 Buoyancy in rapidly rotating fluids

Aircraft reconnaissance measurements have shown that the eye of a mature tropical cyclone is the warmest place in the storm, warmer indeed than the eyewall clouds (Hawkins and Rubsam 1968; Hawkins and Imbembo 1976). From a fluid dynamics perspective, the question then arises: are the eyewall clouds buoyant? The balanced vortex, itself, has *system buoyancy* in the traditional sense when the reference density is set to that of the far field environment. However, the eyewall clouds are not buoyant in the vertical in the traditional sense because air parcels rising in the eyewall have temperatures less than those in the eye (one side of the cloud "environment")! As shown by Smith et al. (2005), the issue is resolved when one defines *local buoyancy* relative to the density distribution of the axisymmetric balanced vortex as in section 2.3.

3 Tropical cyclone intensification and structure

Tropical cyclones are generally highly asymmetric during their intensification phase and only the most intense storms exhibit a strong degree of axial symmetry and, even then, only in their inner-core region. Observations show that rapidly-developing storms are accompanied by "bursts" of deep moist convection, presumably driven by significant local buoyancy (e.g. Heymsfield et al. 2001). The deep convection is maintained by appreciable moisture fluxes at the ocean-air interface, which sustain a conditionally-unstable thermodynamic environment.

In a recent review paper, Montgomery and Smith (2014) examined and compared the four main paradigms that have been proposed to explain tropical cyclone intensification in the *prototype problem for intensification* (see section 1). The four paradigms include: (1) the CISK[1] paradigm; (2) the cooperative intensification paradigm; (3) a thermodynamic air-sea interaction instability paradigm (widely known as WISHE[2]); and (4) a rotating convection paradigm (see Montgomery and Smith 2014 for references).

The first three paradigms assume axisymmetric flow about the rotation axis and therefore no azimuthal eddy terms. This axisymmetric configuration with its attendant phenomenology of axisymmetric convective rings has certain intrinsic limitations for understanding the intensification process (Persing et al. 2013), which, as noted in section 2.6 is quite asymmetric at the cloud scale. As discussed in Montgomery and Smith (2014), the CISK paradigm has a number of well-known issues and it will not be discussed here.

3.1 The cooperative intensification paradigm

What might be regarded as the classical view of tropical cyclone intensification, the cooperative intensification paradigm, emerged from a simple axisymmetric model for intensification formulated by Ooyama (1969). It assumes that the broad-scale aspects of a tropical cyclone may be represented by an axisymmetric, balanced vortex in a stably stratified, moist atmosphere. Balance means that the primary circulation is governed approximately by the thermal wind equation obtained in section 2.2, even in the presence of non-conservative forcing processes such as diabatic heating and friction, which tend to drive the flow away from balance. Under such circumstances, the streamfunction for the axisymmetric, secondary (overturning) circulation required to maintain balance satisfies a second-order partial differential equation, the so-called Sawyer-Eliassen equation. The traditional vortex balance equations are obtained from Eqs. (1)-(6) by retaining the axisymmetric limit of Eqs. (2) and (5) together with the simplified equations given by the underlined terms in Eqs. (1), (3) and (4). See Montgomery and Smith (2014) [pp39-41] for further details.

The cooperative intensification paradigm was explained succinctly by Ooyama (1969)[p18]: "If a weak cyclonic vortex is initially given, there will be organised convective activity in the region where the frictionally-induced inflow converges. The differential heating due to the organised convection introduces changes in the pressure field, which generate a slow transverse circulation

[1]Conditional Instability of the Second Kind.
[2]Wind Induced Surface Heat Exchange.

in the free atmosphere in order to re-establish the balance between the pressure and motion fields. If the equivalent potential temperature of the boundary layer is sufficiently high for the moist convection to be unstable, the transverse circulation in the lower layer will bring in more absolute angular momentum than is lost to the sea by surface friction. Then the resulting increase of cyclonic circulation in the lower layer and the corresponding reduction of the central pressure will cause the boundary layer inflow to increase; thus, more intense convective activity will follow." An appraisal of this paradigm was presented by Montgomery and Smith (2014) [pp45-46] and an extension thereof is discussed in section 3.4. Presumably, the conclusion that "more intense convective activity will follow" is related to the closure scheme adopted for his representation of deep convection[3], which assumes that all the air that converges in the boundary layer is ventilated by the eyewall convection given that some degree of instability is maintained.

3.2 The WISHE paradigm

The WISHE paradigm for intensification is based on the idea of an air-sea interaction instability comprising a postulated multi-step feedback loop involving, in part, the near-surface wind speed and the evaporation of water from the underlying ocean, with the evaporation rate being a function of wind speed and thermodynamic disequilibrium (Emanuel et al. 1994, Emanuel 1997, 2003, 2012). A schematic of this feedback mechanism is shown in Montgomery and Smith (2014) (Fig. 6). In some subcircles, however, the term "WISHE mechanism" is being used more loosely as simply the bulk-aerodynamic transfer of moist enthalpy from the ocean to the atmosphere by the local prevailing winds. When used in this way, it does not constitute a mechanism of vortex intensification. While the WISHE mechanism viewed as a feedback loop is widely held to be "the explanation" as to how tropical cyclones intensify, it has been shown that when the mechanism is suppressed in models by capping the wind speed dependence of the heat fluxes, the vortices still intensify. Therefore the mechanism is unnecessary to explain intensification in the prototype problem, but the simulated vortices do become stronger when the wind-speed dependence of the heat fluxes is retained (Montgomery et al. 2009, 2015).

3.3 The rotating convection paradigm

The rotating convection paradigm recognizes the presence of localized, rotating deep convection that grows in the cyclonic rotation-rich environment of the incipient storm, structures that are intrinsically three-dimensional. The paradigm recognizes also the stochastic nature of deep convection, which has implications for the predictability of local asymmetric features of the developing vortex. The convective updraughts greatly amplify the vertical vorticity locally by vortex-tube stretching and the patches of enhanced cyclonic vorticity subsequently aggregate to form a central monolith of cyclonic vorticity. An azimuthally-averaged view of this paradigm constitutes an extension of the cooperative intensification paradigm in which the boundary layer and eddy processes can contribute positively to producing the maximum tangential winds of the vortex.

In the context of the rotating convection paradigm, an important question arises as to whether there are important differences between three-dimensional tropical cyclones and their purely axisymmetric counterparts? A hint that there may be follows from a finding by Moeng et al. (2004) of an excessive convective entrainment rate in a two-dimensional planetary boundary layer with vertical shear relative to a three-dimensional model. Their results suggest a hypothesis that in the tropical cyclone context, axisymmetric convection occurring in concentric rings is likewise overly efficient in generating buoyancy fluxes compared to three-dimensional convection in isolated thermals, thereby leading to excessive condensation heating and an overly rapid spin-up. Support for this hypothesis was obtained by Persing et al. (2013) in explicit comparisons between three-dimensional and axisymmetric simulations of tropical cyclones.

Before reviewing the salient features of the rotating convection paradigm and its azimuthally-averaged view in detail, it is first necessary to review the dynamics and thermodynamics of the frictional boundary layer.

3.4 Boundary layer dynamics

The boundary layer[4] plays an important role in the dynamics and thermodynamics of tropical cyclones and is an essential component of all the paradigms for intensification referred to above. A brief review of the essentials is necessary here to discuss these paradigms further (see sections 3.5 and 3.6).

Reinforced by the situation in many simple fluid flows, where the boundary layer is one in which the flow speed is reduced by friction to below the free stream value (Schlichting 1968), it has been widely (and reasonably) assumed that friction acts everywhere to reduce the wind speed in a tropical cyclone (see Montgomery and Smith 2014, p56). However, the maximum tangential wind speed in a tropical cyclone is found to occur within the inner core boundary layer (Zhang et al. 2001; Smith et al. 2009). The reasons for this surprising behaviour were anticipated long ago by Anthes (1972) and further elucidated by Smith (2003), Smith and Vogl (2008) and Smith et al. (2009).

[3] Alternative closures in a minimal tropical cyclone model are discussed by Zhu *et al.* (2001).

[4] Loosely defined, the frictional boundary layer is a surface-based layer in which the effects of the turbulent transfer of momentum to the surface are important. Issues surrounding attempts to define this layer more precisely are discussed in Smith and Montgomery (2010); Zhang et al. (2011); Kepert et al. (2016) and Abarca et al. (2015).

As a preliminary for understanding the role of the boundary layer and the surprising behaviour referred to above, it is insightful to consider the spin down of the freely spinning vortex discussed in section 2.2. A scale analysis of the momentum equations (1)-(3) for a boundary layer in general indicates that the pressure gradient force is transmitted approximately unchanged through the boundary layer to the surface (see, e.g. Jones and Watson 1963). In the case of a balanced vortex, the free stream pressure gradient per unit mass is just the sum of the centrifugal and Coriolis forces (C) (section 2.2). Beyond some radius outside the radius of maximum gradient wind, C is reduced in the boundary layer because of the frictional retardation of the tangential wind, v. Thus the radial component of agradient force[5], F_{ar}, is negative and, because v decreases towards the surface, F_{ar} has maximum magnitude at the surface. At these outer radii, the boundary layer flow is *subgradient* and the negative agradient force (the radial component of the first term on the right of Eq. (9)) generates inflow in the boundary layer with the largest inflow near the surface.

As air parcels converge in the boundary layer, they lose absolute angular momentum, M, to the surface. However, if the rate of loss of M is sufficiently small, i.e. less than the rate of decrease in radius, the corresponding tangential velocity (given by $v = M/r - \frac{1}{2}fr^2$) may increase so that at some inner radii, the tangential wind speed in the boundary layer *exceeds* the local value above the boundary layer. We refer to this process as the boundary layer spin up mechanism. At such radii, $F_{ar} > 0$ and the boundary-layer flow is *supergradient*. Then, all forces in the radial momentum equation are outward and the radial inflow rapidly decelerates, leading to upflow at the top of the boundary layer. For these reasons, the boundary layer exerts a strong control on the radii at which the inflow turns up into the eyewall clouds (see e.g. section 3.8). Observational support for the occurrence of the maximum tangential wind within the boundary layer is provided by Kepert (2006a,b); Bell and Montgomery (2008); Montgomery et al. (2014) and Sanger et al. (2014). Support for the boundary layer spin up mechanism is provided by numerical model studies in idealized axisymmetric (Nguyen et al. 2002; Schmidt and Smith 2015) and three-dimensional (Smith et al. 2009; Persing et al. 2013; Abarca and Montgomery 2013; Zhang and Marks 2015) configurations and in numerical simulations of real cases (Zhang et al. 2001). The mechanism is not found in models that use an overly diffusive boundary layer scheme (Smith and Thomsen 2010).

[5]As we have defined it, the agradient force is a measure of the *effective* pressure gradient force, but an alternative definition might include frictional forces also.

3.5 Spin down, spin up and an extended cooperative intensification paradigm

If friction were the only effect acting on a vortex, the boundary-layer would induce radial outflow in a layer above it and the vortex would spin down as air parcels move to larger radii while conserving their absolute angular momentum. This mechanism of vortex spin down was articulated by Greenspan and Howard (1963). If the air in the vortex is stably stratified (as in a tropical cyclone), the vertical extent of the outflow will be restricted by the static stability. Clearly, for a vortex to spin up, there must be some mechanism to produce strong enough inflow *above the boundary layer* to reverse the outflow that would be produced there by the boundary layer alone. The only physically conceivable process capable of producing such inflow in a tropical cyclone is the collective effect of buoyant deep convection in the inner region of the vortex as envisaged in the cooperative intensification paradigm (section 3.1). Typically, a region of deep convection produces an overturning circulation with inflow towards it in the lower half of the troposphere and outflow in the upper half. Put another way, for the vortex to spin up, the convective mass flux must be more than strong enough to *ventilate* the mass that is converging in the boundary layer, thereby overpowering the tendency of the boundary-layer to induce outflow above it.

In the early stages of tropical cyclone intensification, when the primary circulation of the vortex is comparatively weak, the boundary-layer induced inflow and outflow will be weak and the secondary circulation will be dominated by the convectively-induced inflow throughout the lower troposphere. Above the boundary layer, where to a first approximation M is materially conserved, the vortex will spin up. In these stages, the flow in the boundary layer is largely subgradient. However, as the primary circulation increases in strength, the boundary-layer induced convergence will progressively increase, ultimately leading to a spin up of the maximum tangential winds within the boundary layer as described above. Moreover, the convectively-induced inflow may become progressively unable to oppose the low-level outflow induced by the boundary layer; i.e, the convection will become less able to ventilate the mass converging in the boundary layer, thereby slowing down or reversing the rate of intensification of the vortex.

Apart from the boundary-layer spin up mechanism and its consequences, the foregoing processes broadly constitute the cooperative intensification paradigm as articulated by Ooyama (1969). Panel (a) of Figure 1 shows a schematic of the extended cooperative intensification paradigm, while panel (b) highlights the low-level secondary flow feeding into the eyewall of the vortex. These schematics are consistent with the azimuthal average of fully three-dimensional solutions of the governing fluid dynamical equations (e.g. Smith et al. 2009) and with observations (e.g. Montgomery et al. 2014).

A specific illustration of the primary and secondary circulation of a simulated tropical cyclone vortex undergoing intensification in a state-of-the-art cloud model is

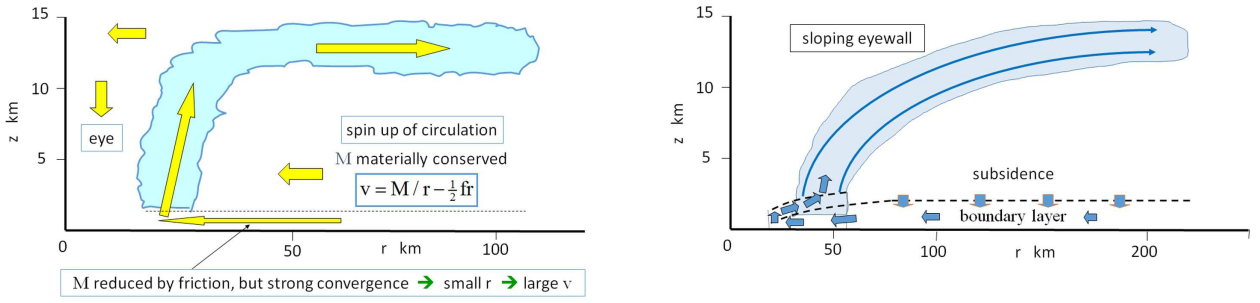

Figure 1. (a) Schematic of the axisymmetric view of tropical cyclone intensification in the new paradigm. Above the boundary layer, spin up of the vortex occurs as air parcels are drawn inwards by the inner-core convection. Air parcels spiralling inwards in the boundary layer may reach small radii quickly (minimizing the loss of absolute angular momentum, M, during spiral circuits) and acquire a larger tangential wind speed v than that above the boundary layer. (b) Schematic of the hurricane inner-core region during intensification in relation to the broader scale overturning circulation. Air subsides into the boundary layer at large and moderate radii and ascends out of the boundary layer at inner radii. The frictionally-induced net inward force in the boundary layer produces a radially inward jet. The subsequent evolution of this jet depends on the bulk radial pressure gradient that can be sustained by the mass distribution at the top of the boundary layer. The jet eventually generates supergradient tangential winds whereafter the radial inflow rapidly decelerates. As it does so, the boundary layer separates and the flow there turns upwards and outwards to enter the eyewall. As this air ascends in the eyewall, the system-scale tangential wind and radial pressure gradient come into gradient wind balance. This adjustment region has the nature of an unsteady centrifugal wave with a vertical scale of several kilometres, akin to the vortex breakdown phenomenon (Rotunno (2014) and refs.)

shown in Fig. 2, taken from Persing et al. (2013). Noteworthy features of the azimuthally-averaged flow are as follows. There is weak inflow through much of the lower troposphere with strong inflow in a shallow boundary layer and a strong outflow just above it where the flow erupts into the eyewall. There is outflow also in the upper troposphere. The maximum tangential wind is found within the layer of strong inflow. Above this height, the tangential wind decreases with height and the radius of the maximum tangential wind at a given height increases with increasing height. The vertical velocity field shows a region of strong ascent into the upper troposphere where the boundary layer erupts into the interior vortex. This updraught region is essentially moist saturated (not shown) and the inner edge of this cloudy region is referred to as the eyewall of the storm. Inside and outside of the main updraught region, there is weak subsidence. Near the top of the boundary layer where the flow turns into the eyewall updraught, there is a secondary maximum of vertical velocity.

As the vortex intensifies, the boundary layer exerts an ever increasing control on the pattern of convection as well as on the ability of the convection to ventilate the mass that is converging in the boundary layer (Ooyama, 1982). Accordingly there is a subtle interplay through boundary layer dynamics between the spin up of the circulation above the boundary layer, which depends on the strength and location of the convection, and the boundary layer response, which exerts a control on the radii at which air ascends. The fate of the ascending air depends in part on thermodynamic processes, which affect the ability of convection to evacuate the increasing mass flux within the boundary layer and continue to produce inflow above the boundary layer (Kilroy et al. 2015; Schmidt and Smith 2015).

3.6 Boundary layer thermodynamics

Ooyama's articulation of the cooperative intensification paradigm assumed that the boundary layer θ_e would remain high enough to sustain deep convection as the vortex developed (section 3.1). In his model, the required high θ_e values were sustained by wind-speed dependent surface moisture fluxes. In the WISHE paradigm, spin up depends crucially on a progressive increase of the surface moisture fluxes with wind speed (see e.g. Montgomery and Smith 2014, Fig. 6).

As in the cooperative intensification paradigm, the rotating convection paradigm for spin up requires a modest elevation of low-level moisture and hence θ_e to sustain deep convection at radii where air is being lofted from the boundary layer into the eyewall. For reasons discussed above, the maintenance of buoyant deep convection is a prerequisite[6] for the convection to ventilate the increasing amount of air being lofted from the boundary layer as the vortex intensifies and the upper-level warm core aloft strengthens (Kilroy et al. 2015).

3.7 Outer-core size

From a forecasting perspective, the prediction of tropical cyclone size (i.e. the extent of gale force winds, speeds greater than 17 m s^{-1}) is comparable in importance with the prediction of intensity. For example, Atlantic

[6]The ability of deep convection to ventilate the mass that is expelled by the boundary layer depends on the convective mass flux, and the mass flux must depend *inter alia* on the buoyancy of the cloud updraughts. However, it depends also on the area of the updraughts. Clearly, to gain further insight that is free from speculation about its postulated behaviour, one needs to calculate the changes in convective mass flux using a numerical model (see e.g. Kilroy et al. 2015).

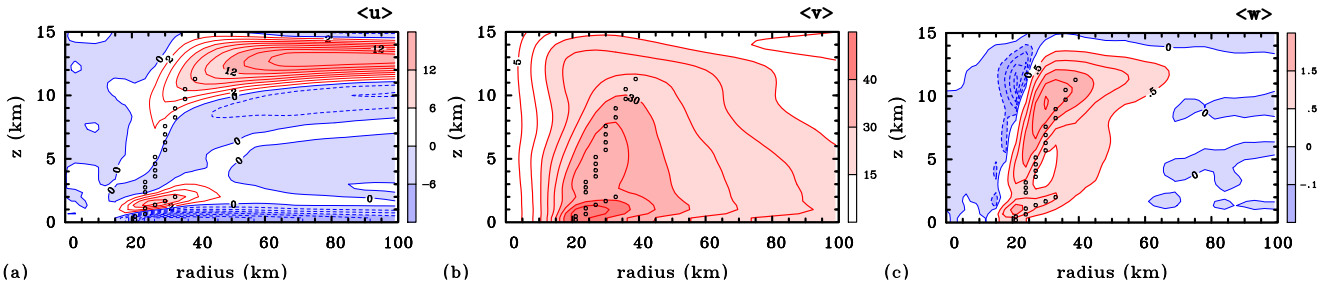

Figure 2. Radius-height cross sections of the azimuthally-averaged velocity components in the simulation described by Persing et al. (2013), time averaged during the mature phase (144-148 h) of the three-dimensional calculation. (a) radial velocity (contour interval 2 m s^{-1}, (b) tangential velocity (contour interval 5 m s^{-1}), (c) vertical velocity (contour interval 0.5 m s^{-1} for positive values, 0.1 m s^{-1} for positive values). Positive values red/solid, negative values blue/dashed, shading levels as indicated by the side bar. The dotted curve in each plot shows the location of the maximum tangential wind speed at each height.

Hurricane Sandy (2012) was only a Category 3 storm, but was accompanied by an enormous area of gales that led to extensive damage along the United States east coast. The practical importance of the size problem has motivated a number of theoretical and numerical studies examining factors that determine tropical cyclone size (e.g., Yamasaki 1968; Rotunno and Emanuel 1987; DeMaria and Pickle 1988; Xu and Wang 2010; Smith et al. 2011; Rappin et al. 2011; Li et al. 2012; Hakim 2011; Chan and Chan 2014; Chavas and Emanuel 2014; Frisius 2015; Kilroy et al. 2015). An appraisal of many of these studies is given by Kilroy et al. (2015).

An underlying assumption of most of these studies is that there exists a global quasi-steady solution for storms, an assumption that would require, *inter alia*, that the storm environment be quasi steady. This requirement is unlikely (see section 6). In fact, according to the conventional paradigm for tropical cyclone intensification (section 3.5), one would anticipate that the outer circulation will expand as long as the aggregate effect of deep convection [including the eyewall and convective rainbands (Fudeyasu and Wang 2011)] remains strong enough to maintain the inward migration of absolute angular momentum surfaces. As demonstrated by Kilroy et al. (2015), the broadening circulation has consequences for the boundary layer dynamics, which play a role in determining the radii at which air ascends into the eyewall and the maximum tangential wind speed, which occurs within the boundary layer (section 3.4). The broadening circulation has consequences also for the boundary layer thermodynamics, which affects the spatial distribution of diabatic heating above the boundary layer (section 3.6).

3.8 Boundary layer control on inner-core size

Kilroy et al. (2015) examined the long-term behaviour of tropical cyclones in the prototype problem for cyclone intensification on an f-plane using a nonhydrostatic, three-dimensional numerical model. After reaching a mature intensity, the model storms progressively decay while both the inner-core size, characterized by the radius of the eyewall, and the size of the outer circulation (measured for example by the radius of gale-force winds) progressively increase. This behaviour was explained in terms of a boundary layer control mechanism in which the expansion of the swirling wind in the lower troposphere leads through boundary layer dynamics to an increase in the radii of forced eyewall ascent as well as to a reduction in the maximum tangential wind speed in the layer. These changes are accompanied by ones in the radial and vertical distribution of diabatic heating, which, influences the inflow in the lower troposphere and thereby the expansion of the swirling wind in the lower troposphere.

Kilroy et al. (2015) pointed out that the tight coupling between the flow above the boundary layer and that within the boundary layer makes it impossible, in general, to present simple cause and effect arguments to explain vortex behaviour. The best one can do is to articulate the individual elements of the coupling, which might be described as a set of coupled mechanisms. They employed a simple, steady, slab boundary layer model (detailed in Smith et al. 2015), as a way to break into the chain of coupled mechanisms referred to above. The assumption is that, because the boundary layer is relatively shallow, it adjusts rapidly to the flow above it. Since the partial differential equations from which the slab boundary layer model is derived are parabolic in the radially inward direction, the inflow and hence the ascent (or descent) at the top of the boundary layer at a given radius R knows only about the tangential wind profile at radii $r > R$ (see Fig. 3). The inflow at radius R knows nothing directly about the vertical motion at the top of the boundary layer at radii $r < R$, including the pattern of ascent into the eyewall cloud associated with convection under the eyewall. In contrast, the numerical simulation does not solve the boundary layer equations separately, and it does not make any special boundary layer approximation. Thus, the ability of the slab boundary layer model to produce a radial distribution of radial, tangential and vertical motion close to those in the time-dependent numerical simulation provides a useful measure of the degree of boundary layer control in the evolution of the vortex.

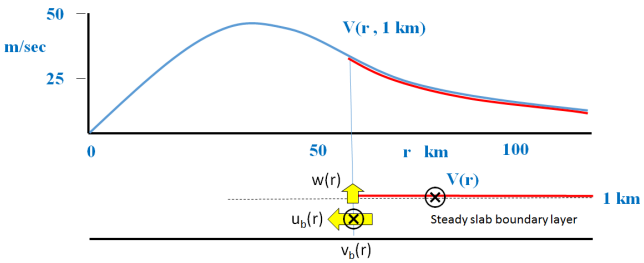

Figure 3. Schematic illustrating the idea behind the boundary layer control mechanism.

As an example, we show in Fig. 4 a comparison of velocity fields from the slab boundary layer calculations compared with the corresponding azimuthally-averaged fields from the full numerical simulation at latitude 20^{o}N. The radial and tangential wind components from the numerical simulation are averaged over the lowest 1-km depth, corresponding to an average over the depth of the boundary layer, to provide a fair comparison with the slab boundary layer fields. The slab boundary layer calculations are performed every 12 h using the smoothed, azimuthally-averaged tangential wind profile extracted from the numerical simulation shown in Kilroy et al. (2015) (their Fig. 5). Even though the integration of the slab boundary layer equations breaks down at some inner radius, where the radial velocity tends to zero and the vertical velocity becomes large, the calculations capture many important features of the corresponding depth-averaged boundary layer fields from the numerical simulations. For example, they capture the broadening of the vortex core with time, i.e., the increase in the radii of maximum tangential wind speed and eyewall location, the latter characterized by the location of maximum vertical velocity. They capture also the broadening of the outer radial and tangential wind field. However, they overestimate the radial extent of the subsidence outside the eyewall (cf. Figs. 4e,f). For reasons articulated above, these results provide strong support for the existence of a dynamical control by the boundary layer on the evolution of the vortex. Kilroy et al. (2015) investigated also the thermodynamic control of the boundary layer and other aspects of the coupling discussed above.

The Kilroy et al. study provides new insight on the factors controlling the evolution of the size and intensity of a tropical cyclone as well as a plausible and simpler explanation for the expansion of the inner core of Hurricane Isabel (2003) and Typhoon Megi (2010) than given previously.

3.9 Eyewall spin up

Schmidt and Smith (2015) developed an improved version of a minimal axisymmetric model for a tropical cyclone and used it to revisit some fundamental aspects of vortex behaviour in the prototype problem for tropical cyclone intensification. The calculation highlights, *inter alia*, the pivotal role of the boundary layer in spinning up the tangential winds in the eyewall updraught. As discussed in section 3.4, the spin up in the boundary layer is associated with the development there of supergradient winds. The spin up of the eyewall updraught occurs by the vertical advection of the high tangential momentum associated with the supergradient winds in the boundary layer. These boundary layer and eyewall spin up mechanisms, while consistent with some recently reported results (e.g. Kilroy et al. 2015), are not part of the classical theory of tropical cyclone spin up (see section 3.1). In fact, in the eyewall updraught, the flow is outwards (typifying the outward slope of the eyewall) so that the radial advection of absolute angular momentum (or radial flux of absolute vorticity) makes a *negative contribution* to spin up in this region. Even so, there is inflow in the middle layer at large radii where the classical mechanism operates to spin up the tangential winds. Based on the results of Kilroy et al. (2015), the spin up at large radii, where the flow in the boundary layer is subgradient, leads to a feedback on the inner-core vertical motion through boundary-layer dynamics and to a change in the spatial distribution of diabatic heating, mostly above the boundary layer, through boundary layer thermodynamics.

3.10 Efficiency arguments

Following pioneering studies of Schubert and Hack (1982), Hack and Schubert (1986) and Vigh and Schubert (2009) in the context of the inviscid, axisymmetric, balance equations forced by a prescribed diabatic heating, there are widely-held arguments that attribute the increasingly rapid intensification of tropical cyclones to the increasing "efficiency" of diabatic heating in the cyclone's inner core region associated with deep convection (e.g. Vigh and Schubert 2009; Rozoff et al. 2012). The efficiency, in essence the amount of temperature warming compared to the amount of latent heat released, is argued to increase as the vortex strengthens on account of the strengthening inertial stability. Assuming that the diabatic heating rate does not change, the strengthening inertial stability progressively weakens the secondary circulation, which, in turn, is argued to reduce the rate of adiabatic cooling of rising air. Thus more of the heating is available to raise the temperature of the air parcel. Another aspect of the efficiency ideas concerns the location of the heating in relation to the radius of maximum tangential wind speed, with heating inside this radius seen to be more efficient in developing a warm core thermal structure and, presumably, an increase in tangential wind.

Recently, Smith and Montgomery (2015) provided a more direct interpretation of the increased spin up rate when the diabatic heating is located inside the radius of maximum tangential wind speed. Further, they drew attention to the limitations of assuming a fixed diabatic heating rate as the vortex intensifies and, on these grounds alone,

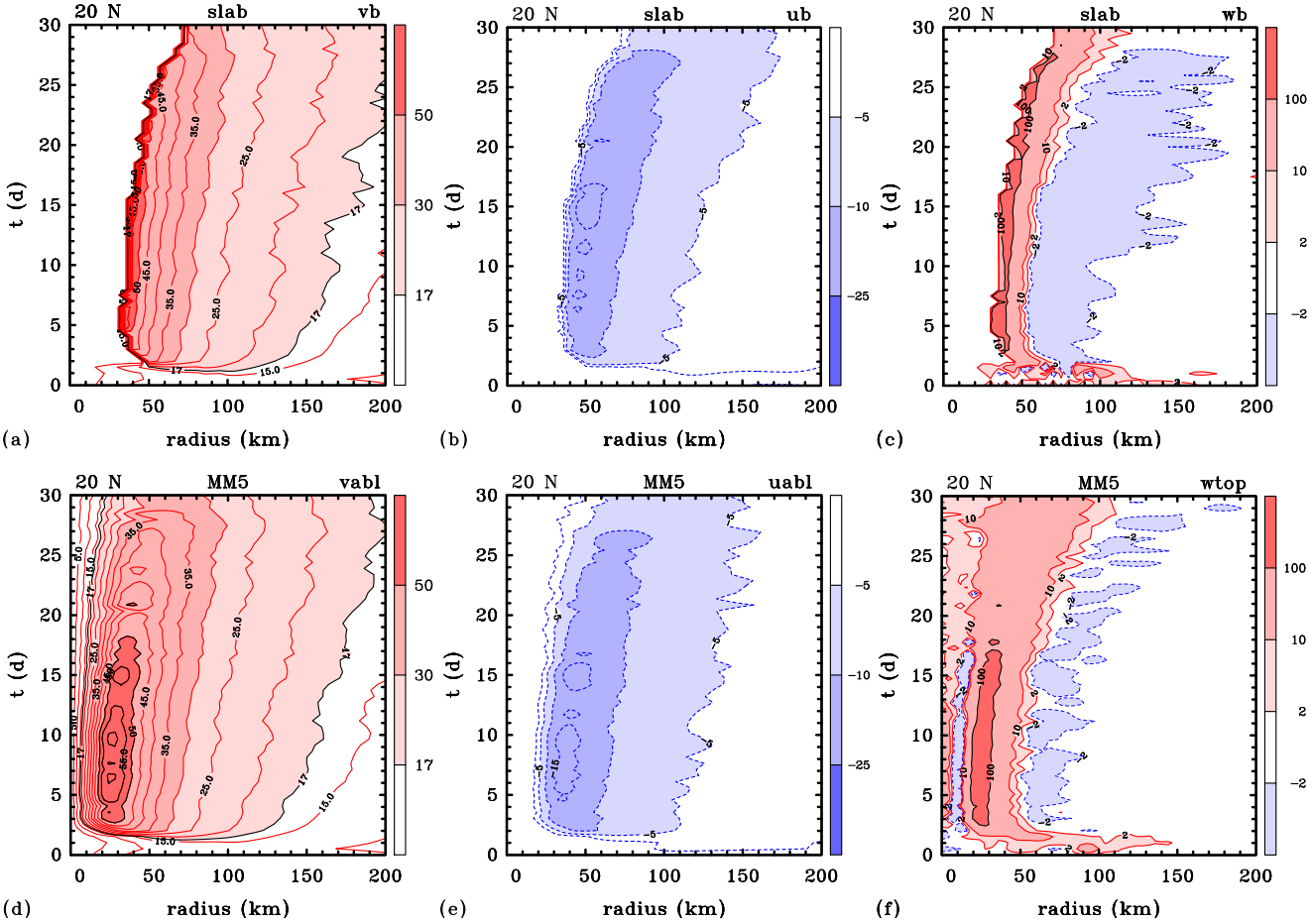

Figure 4. The upper panels show Hovmöller plots of tangential and radial velocities in the boundary layer and the vertical velocitiy at the top of the boundary layer from the slab boundary layer model, with a constant depth of 1000 m. The lower panels show the corresponding azimuthally-averaged and temporally-smoothed quantities from the MM5 output. Contour interval: (a),(b),(d),(e) 5 m s^{-1}; (c),(f): ± 2 cm s^{-1}, 10 cm s^{-1}. The 17 m s^{-1} contour is shown also in (a) and (d), the -2 m s^{-1} contour in (b) and (e), and the 1 m s^{-1} contour in (c) and (f). Solid contours positive, dashed contours negative. Colour shading levels as indicated. Adapted from Kilroy et al. (2015).

they offered reasons why it is questionable to apply the efficiency arguments to interpret the results of observations or numerical model simulations of tropical cyclones. Since the spin up of the maximum tangential winds in a tropical cyclone takes place in the boundary layer and the spin up of the eyewall is a result of the vertical advection of high angular momentum from the boundary layer, Smith and Montgomery questioned whether deductions about *efficiency* in theories that neglect the boundary layer dynamics and thermodynamics are relevant to reality. The efficiency idea was discussed (but not endorsed) in a multiscale analysis of the rapid intensification of Hurricane Earl (2010) by Rogers et al. (2015).

4 More on the rotating convection paradigm

As noted in section 3.3, the findings of Persing et al. (2013) suggest that previous studies using strictly axisymmetric models and their attendant phenomenology of axisymmetric convective rings have intrinsic limitations for understanding the intensification process. To further understand the role of eddy dynamics during tropical cyclone intensification, we return now to examine the rotating convection paradigm in more detail. There is accumulating observational evidence supporting the hypothesis that convective bursts in pre-depression disturbances and tropical cyclones act to spin up localized cyclonic vorticity anomalies in the lower troposphere (Reasor et al. 2005; Sippel et al. 2006; Bell and Montgomery 2010; Raymond and Carillo 2011; Sanger et al. 2014; Kilroy and Smith 2015). The question then arises: what is the role of these cyclonic vorticity anomalies in the spin up process and what way might they modify the azimuthally-averaged view of the rotating convection paradigm?

4.1 Role of cloud-generated vorticity

To help motivate one of the issues involved in understanding the role of in-cloud vorticity in the dynamics of a developing tropical cyclone, recall Stokes' theorem, which equates the area-integrated vertical vorticity to the circulation defined by the line integral around a closed circuit loop

within the fluid on a horizontal height surface. At any given instant in time, the circulation is, of course, given by the area-integrated vorticity within the loop. Vortical convective processes occurring within the loop, such as adiabatic vortex merger (Melander et al. 1988; Dritschel and Waugh 1992; Lansky et al. 1984), vortex axisymmetrization processes (Melander et al. 1988; Montgomery and Enagonio 1998), and diabatic modifications thereof (Hendricks et al. 2004; Tory et al. 2006), while certainly contributing to the consolidation and upscale growth of cyclonic vorticity within the loop, would seem to be unimportant to the net circulation unless these processes have an influence on the flow normal to the loop.

In general, the *change in circulation* (and vorticity) is governed by the divergence of a horizontal flux, and the flux is comprised of an advective and a non-advective contribution (Haynes and McIntyre 1987). For the purposes of this discussion we adopt standard geometric coordinates with z denoting height above the ocean surface. The equation for the local tendency of absolute vertical vorticity ζ_a may be written as

$$\frac{\partial \zeta_a}{\partial t} = -\nabla_h \cdot \mathbf{F}_{\zeta_\mathbf{a}}, \qquad (11)$$

where $\mathbf{F}_{\zeta_\mathbf{a}} = \mathbf{F_{af}} + \mathbf{F_{naf}}$, $\mathbf{F_{af}} = \mathbf{u_h}\zeta_a$ and $\mathbf{F_{naf}} = -\zeta_\mathbf{h} w + \mathbf{k} \wedge \mathbf{F_{fri}}$. Here $\mathbf{u_h}$ is the horizontal velocity vector, $\zeta_\mathbf{h}$ is the horizontal vorticity vector, w is the vertical velocity, $\mathbf{F_{fri}}$ is the horizontal force per unit mass due to molecular effects and sub-grid-scale eddy momentum flux divergences, and $\mathbf{k}$ is a unit vector in the vertical. In this form of the vertical vorticity equation, the baroclinic term that would ordinarily appear as an additional term on the right hand side of Eq. (11) is neglected because this term is generally very small in the tropics (Raymond et al. 2014). From these definitions, it follows that the advective flux is given by $\mathbf{F_{af}}$ and the non-advective flux is given by $\mathbf{F_{naf}}$. The non-advective flux is associated with vortex-tube-tilting processes as well as friction associated with sub-grid-scale eddy momentum transfer.

The physics of the non-advective fluxes is described elegantly by (Raymond et al., 2014, their Fig. 1). The foregoing formalism is mathematically equivalent to the material form of the equation for the vertical vorticity (e.g. Batchelor 1967; Holton 2004)[7]. The material form of the vorticity equation does not explicitly convey the area-integrated constraint contained by the flux form expressed by Eq. (11). In contrast, calculating the divergence of the advective flux does not distinguish between local changes in vorticity associated with pure advection and the generation of vorticity by stretching. One would need to calculate the stretching effect separately (see e.g. Raymond and Carillo 2011, p156, column 2).

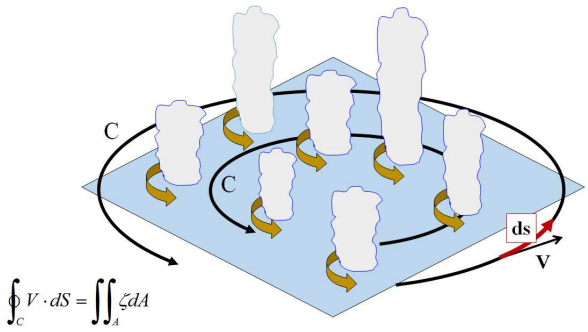

Figure 5. Schematic of a region of deep rotating updrafts with two hypothetical circuits indicated by circles. By Stokes' theorem, the circulation about either circle is equal to the areal integral of the vorticity enclosed by that circuit. See text for further discussion.

For the simple thought experiment posed here (see Fig. 5), the loop is first imagined to lie outside of the convecting region and thus the non-advective contribution to the net circulation tendency is negligible compared to the advective vorticity flux. In this situation, the key factor responsible for changing the net circulation is the flux of absolute vorticity across the loop. In an azimuthally-averaged viewpoint phrased with respect to an approximate invariant centre of circulation, there will be both axisymmetric (or "mean") and non-axisymmetric (or "eddy") contributions to the absolute vorticity flux across the loop. If, on the other hand, the loop resides within the convective region, the non-advective flux contribution around the loop may no longer be small in regions where there is mean ascent or localized ascent that is spatially correlated with horizontal vorticity. Recent findings summarized in section 4.2 show that eddy processes in the active cumulus zone of a developing vortex contribute positively to both the advective and non-advective fluxes of vorticity and therefore contribute positively to the amplification of system-scale circulation there. More will be said about this in section 4.2.

4.2 Role of cloud-scale eddies

Motivated by the foregoing discussion regarding in-cloud vertical vorticity and the associated flux form of the vertical vorticity equation, we summarize now recent findings using near cloud-resolving, three-dimensional simulations of an intensifying tropical cyclone. To this end, we integrate the vorticity equation (11) over a horizontal circle of radius r, radius being defined relative to an instantaneous centre of circulation. Then, dividing by $2\pi r$, one obtains the equation for the azimuthally-averaged tangential velocity tendency

[7] The material form proves useful in understanding the *local amplification* of vorticity following fluid parcels by deep convective updraughts, in contrast to the *concentration* of vorticity inferred from Eq. (11) within a fixed closed circuit (assuming of course that $-\nabla_h \cdot \mathbf{F}_{\zeta_\mathbf{a}} > 0$). It is only the concentration of vorticity that leads to an increase of circulation about a fixed circuit. The local amplification of vorticity does not, by itself, increase the circulation because the increase of vorticity by stretching is accompanied by a decrease in the area of the material vortex tube that is stretched with zero change of circulation about this material circuit. However, by mass continuity, stretching must be accompanied by flow convergence across the fixed circuit, which, if $-\nabla_h \cdot \mathbf{F}_{\zeta_\mathbf{a}} > 0$, does lead to an increase in circulation about this circuit.

(i.e., the azimuthal average of Eq. (2)):

$$\frac{\partial \langle v \rangle}{\partial t} = \underbrace{-\langle u \rangle \langle f+\zeta \rangle}_{V_{m\zeta}} \underbrace{-\langle w \rangle \frac{\partial \langle v \rangle}{\partial z}}_{V_{mv}} \underbrace{-\langle u'\zeta' \rangle}_{V_{e\zeta}} \underbrace{-\left\langle w' \frac{\partial v'}{\partial z} \right\rangle}_{V_{ev}} \underbrace{-c_p \left\langle \frac{\theta'_\rho}{r} \frac{\partial \pi'}{\partial \lambda} \right\rangle}_{V_{ppg}} + \underbrace{\langle D_v \rangle}_{V_d} \quad (12)$$

Here and elsewhere, the prime denotes a departure from the azimuthal mean (or "eddy"). The azimuthal average of some quantity Q, denoted by the bracket symbol, is defined by $\langle Q \rangle (r,z,t) = \frac{1}{2\pi}\int_0^{2\pi} Q(r,\lambda,z,t)d\lambda$, where λ is the azimuth (in radians).

The terms on the right hand side of Eq. (12) are recognized as the azimuthally-averaged advective and non-advective vorticity fluxes in the Haynes and McIntyre form of the vorticity substance equation divided by $2\pi r$ (in geometric coordinates). The mean and eddy terms in Eq. (12) are, respectively, the mean radial influx of absolute vertical vorticity ($V_{m\zeta}$), the mean vertical advection of mean tangential momentum (V_{mv}), the eddy radial vorticity flux ($V_{e\zeta}$), the vertical advection of eddy tangential momentum (V_{ev}), the azimuthal perturbation pressure gradient per unit mass (V_{ppg})[8], and the combined diffusive and planetary boundary layer tendency (V_d). This methodology represents the traditional Eulerian approach to "eddy-mean" partitioning in the tangential wind equation (e.g., Hendricks et al. 2004; Montgomery et al. 2006b; Yang et al. 2007)[9]. This formalism is analogous to a Reynolds averaging of the fluid equations for turbulent flow.

The subgrid-scale diffusive tendency of the tangential wind component may be separated into radial (V_{dr}) and vertical (V_{dz}) contributions:

$$\langle D_v \rangle = \underbrace{\frac{1}{r^2}\frac{\partial \langle r^2 \tau_{r\lambda} \rangle}{\partial r}}_{V_{dr}} + \underbrace{\frac{1}{\rho_0}\frac{\partial \langle \rho_0 \tau_{\lambda z} \rangle}{\partial z}}_{V_{dz}} \quad (13)$$

where the subgrid-scale momentum fluxes are related to the mean strain-rate tensor in cylindrical coordinates by a simple K-theory closure taking the form of local eddy diffusion relations (written here in cylindrical-polar coordinates),

$$\begin{aligned} \langle \tau_{r\lambda} \rangle &= \left\langle K_{m,h} \left(\frac{1}{r}\frac{\partial u}{\partial \lambda} + r\frac{\partial v/r}{\partial r} \right) \right\rangle, \\ \langle \tau_{\lambda z} \rangle &= \left\langle K_{m,v} \left(\frac{1}{r}\frac{\partial w}{\partial \lambda} + \frac{\partial v}{\partial z} \right) \right\rangle \end{aligned} \quad (14)$$

with parameterization formulae for horizontal and vertical eddy diffusivities, $K_{m,h}$ and $K_{m,v}$ (not written here, see Persing et al. 2013 for details.). The analogous specification for $\langle \tau_{rz} \rangle$ is

$$\langle \tau_{rz} \rangle = \left\langle K_{m,v} \left(\frac{\partial u}{\partial z} + r\frac{\partial w/r}{\partial r} \right) \right\rangle. \quad (15)$$

and $\rho_0(z)$ is the basic state density profile. As discussed above, from the viewpoint of the flux form of the vorticity equation, the subgrid-scale turbulent momentum fluxes $\langle \tau_{r\lambda} \rangle$ and $\langle \tau_{\lambda z} \rangle$ are regarded as part of the non-advective vorticity flux.

Persing et al. (2013)[sec. 6] found that, while the mean vorticity influx and vertical advection terms comprise leading terms of the mean tangential wind tendency (thereby supporting the revised spin up schematic of Fig. 1b), the resolved and parameterized (subgrid) eddy processes contribute significantly also to the mean spin-up tendency around the eyewall and tangential wind maximum throughout the troposphere. The resolved eddy momentum fluxes are associated with the in-cloud vorticity structures. Insight into the physical nature of the in-cloud vorticity structures was obtained by Persing et al. (2013) using a flux equivalent form of Eq.(12), adopting a Boussinesq approximation for simplicity. Equation (12) may then be re-written as follows:

$$\begin{aligned} \frac{\partial \langle v \rangle}{\partial t} = &-\frac{1}{r^2}\frac{\partial \left(-r^2 \langle u \rangle \langle v \rangle\right)}{\partial r} - \frac{\partial (\langle w \rangle \langle v \rangle)}{\partial z} - f\langle u \rangle \\ &-\frac{1}{r^2}\frac{\partial \left(r^2 \langle u'v' \rangle\right)}{\partial r} - \frac{\partial (\langle v'w' \rangle)}{\partial z} \\ &+c_p \left\langle \frac{\theta'_\rho}{r}\frac{\partial \pi'}{\partial \lambda} \right\rangle + \langle D_v \rangle . \end{aligned} \quad (16)$$

Again, D_v is the subgrid-scale tendency expressed as a radius-height divergence of the subgrid momentum fluxes τ:

$$\langle D_v \rangle = \frac{1}{r^2}\frac{\partial r^2 \langle \tau_{r\lambda} \rangle}{\partial r} + \frac{\partial \langle \tau_{\lambda z} \rangle}{\partial z} \quad (17)$$

where, for consistency with the Boussinesq-type of approximation, the vertical variation of the basic state density has been neglected in the vertical derivative term in (17). The comparison of (16) and (17) shows the direct analogy of resolved $-\langle u'v' \rangle$ and $-\langle v'w' \rangle$ with subgrid $\langle \tau_{r\lambda} \rangle$ and $\langle \tau_{\lambda z} \rangle$. In addition, in the mean radial and vertical momentum tendency equations (not written), the resolved $-\langle u'w' \rangle$ is the analogue of subgrid $\langle \tau_{rz} \rangle$.

[8] This term is the equivalent representation of the azimuthally averaged perturbation pressure gradient force per unit mass in Eq. (2). The quantity π' is the perturbation Exner function defined as $\pi' = \pi - <\pi>$ with π the Exner function from section 2.1, and $\theta'_\rho = \theta_\rho - <\theta_\rho>$ is the perturbation density potential temperature that accounts for water vapour and cloud water (Emanuel 1994).

[9] Although we do not depart from this approach here, we note that, in principle, highly localized asymmetric features can project upon what are termed here as "mean" terms. For example, if we suppose an otherwise axisymmetric vortex with an imposed, single, large-amplitude, positive anomaly in vertical motion, this anomaly will project onto both the vertical eddy and mean terms.

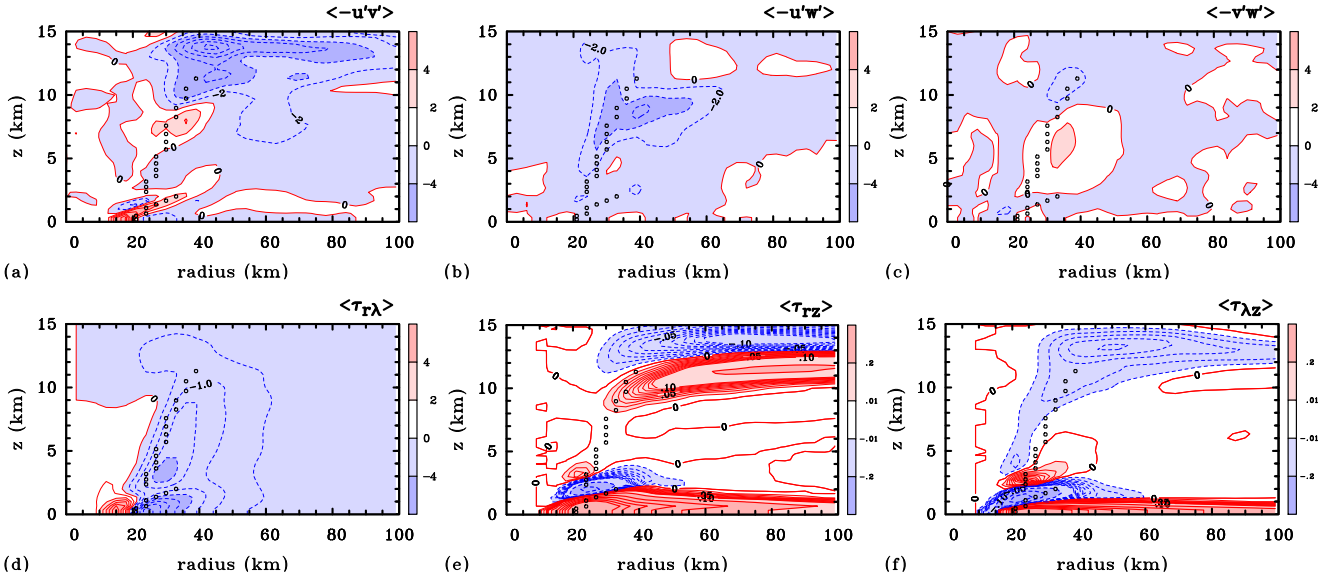

Figure 6. Radius-height contour plots of resolved and subgrid-scale eddy momentum fluxes and related quantities from the 3D3k simulation of Persing *et al.* (2013: their Fig. 15) averaged over the second intensification interval (144 - 148 h). (a) resolved horizontal momentum flux $< -u'v' >$; (b) resolved vertical eddy flux of radial momentum $< -u'w' >$; (c) resolved vertical eddy flux of tangential momentum $< -v'w' >$); (d) subgrid momentum flux corresponding to panel (a), $< \tau_{r\lambda} >$; (e) subgrid momentum flux corresponding to panel (b), $< \tau_{rz} >$; (f) subgrid momentum flux corresponding to panel (c), $< \tau_{\lambda z} >$. Contour interval for panels (a) - (c) is 2 m^2 s^{-2}; for panel (d) 0.5 m^2 s^{-2}; for panels (e) and (f) 0.01 m^2 s^{-2} between -0.1 and +0.1 (thin) and 0.2 m^2 s^{-2} above 0.1 and below -0.1 (thick). The dotted curve in each plot shows the location of the maximum azimuthally averaged tangential wind speed at each height.

4.2.1 *Horizontal eddy momentum fluxes*

Figure 6 shows the horizontal (radial) eddy momentum flux in a radius-height format and is focused on the inner-core region of the vortex where the deep convection is active. Shown also are the corresponding subgrid-scale momentum fluxes parameterized by the turbulence closure scheme given by Eqs. (14) and (15). For reference, the dotted curves in the figures identify the radius of the maximum azimuthally-averaged tangential velocity (hereafter referred to as the RMW) at each height. The data are time-averaged over a four hour interval (144 - 148 h) during an intensification phase of the vortex, but other time intervals during intensification produce similar results.

Figure 6a shows that during spin-up, the resolved-eddy momentum flux, $-\langle u'v' \rangle$, has a coherent region of positive values around the RMW within and just above the boundary layer and extending upwards and outwards in the mean updraught to the middle troposphere. This implies an inward eddy tangential (and angular) momentum transport that is directed in the same sense as the gradient of mean angular velocity (cf. Eq. (14)), which has its maximum value at or near the centre of circulation during the spin up phase. In contrast, Fig. 6d shows that that the corresponding subgrid-scale momentum flux is predominantly negative and much weaker in magnitude than the resolved-eddy flux near the RMW and within the mean updraught. Therefore, the resolved flux in the lower troposphere acts in a direction opposite to the averaged local angular velocity gradient presumed by the subgrid scale model, i.e., it is counter-gradient[10]. Simply, the resolved horizontal eddy momentum flux does not act diffusively to weaken the mean vortex. Rather, it amplifies the low-level tangential winds inside the RMW and contributes to a contracting RMW with time.

Insight into the nature of the up-gradient horizontal eddy momentum fluxes was provided by Persing et al. (their section 6.5), who used high-resolution model output to examine the temporal evolution of the convective vorticity structures in horizontal planes. The evolutionary behaviour of these structures is dominated by deep convection episodes, cyclonic vorticity enhancement by vortex-tube stretching in convective updraughts near the radius of maximum winds, and vortex wave-like dynamics involving the progressive shearing of cyclonic vorticity anomalies.

4.2.2 *Vertical eddy momentum fluxes*

The patterns of the resolved vertical eddy fluxes (i.e., $-\langle u'w' \rangle$ and $-\langle v'w' \rangle$ in Figs. 6b,6c are tall, negative, outward-sloping columns concentrated around the RMW and mean updraught. This location is where the vortical convective updraughts are most active, and they are presumably the primary agents of these flux columns. The tendency of these flux columns contributes to extending the region of strong tangential wind higher in the troposphere.

[10]The azimthally averaged radial subgrid-scale momentum flux (Eq. 14) is dominated by $K_{m,h} r \partial / \partial r (< v > /r)$. Although $K_{m,h}$ does vary with radius and height (see Fig. 15 of Persing et al. 2013), the radial derivative of $< v > /r$ dominates.

Persing et al. (2013) found that the spin-up tendency from V_{ev} (and the corresponding vertical divergence of $-\langle w'v' \rangle$) is roughly three times larger than that for $V_{e\zeta}$. That is, in the region of vortical convection, the contribution from the non-advective eddy vorticity flux to spin up is comparable with, or greater than the contribution from the advective eddy vorticity flux. Persing et al. (2013) found also that the resolved-eddy flux, $-\langle u'w' \rangle$, does not act like eddy diffusion, but rather acts to strengthen locally the mean overturning circulation.

The subgrid vertical fluxes (Figs. 6e,6f) have the expected large extrema in the boundary layer, but they show nothing in the tropospheric RMW-updraught region where the resolved-eddy fluxes are active. There is some pattern similarity in the negative $-\langle v'w' \rangle$ and $\langle \tau_{\lambda z} \rangle$ in the upper-troposphere updraught region, but the latter is much smaller in magnitude. Also, $\langle \tau_{rz} \rangle$ has a weak vertical dipole pattern in the upper-tropospheric outflow region. This pattern implies a weak tendency in $\langle u \rangle$ to decrease the outflow altitude.

4.2.3 *Synthesis and revised spin up cartoon*

In a nutshell, during the spin up of the vortex, the resolved eddy momentum fluxes associated with the cloud-scale eddies act to strengthen the mean tangential and radial circulation in the developing eyewall region. The largest resolved-eddy fluxes occur in the RMW-updraught region where vortical convection is most active. The resolved eddy fluxes generally do not act like eddy diffusion, but represent a non-local flux associated with the vortical updraughts and downdraughts. The resolved eddy component of the non-advective vorticity flux is as important in the vorticity (and circulation) dynamics as the corresponding advective vorticity flux. The foregoing results show that both radial and vertical resolved eddy-fluxes have qualitatively different patterns above the boundary layer compared to the subgrid scale eddy-diffusive fluxes, and the resolved-eddy fluxes are generally larger in magnitude, especially the vertical fluxes. The disparity between the resolved and subgrid patterns belies a simple interpretation as local momentum mixing.

During intensification, the multiple vortical updraughts will excite vortex Rossby and inertia-buoyancy waves (as discussed elsewhere e.g. in Chen et al. 2003; Reasor and Montgomery 2015), which will in turn contribute also to the sign and structure of the eddy momentum fluxes. The intensification process generally comprises a turbulent system of rotating, deep moist convection and vortex waves. A more complete understanding of the complex eddy dynamics is certainly warranted.

The foregoing findings regarding the positive contribution of the eddy processes to vortex spin up have been confirmed recently by Zhang and Marks (2015) using an idealized configuration of the NOAA operational hurricane forecast model. For realistic settings in the subgrid scale parameterizations suggested by recent observations,

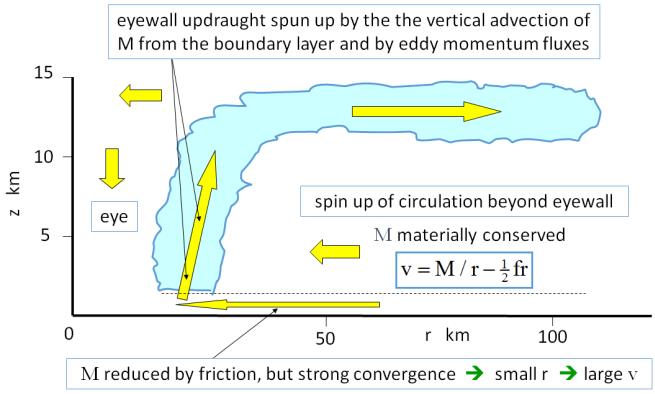

Figure 7. Schematic illustrating the revised view of system-scale spin up in the rotating convection paradigm.

they found (p3992), *inter alia*, that "Angular momentum budget analyses during the intensification phase suggest that the eddy transport of angular momentum contributes substantially to the total tendency of angular momentum, especially at low levels ($<$ 4 km) inside the radius of the maximum tangential wind speed when L_h (the horizontal mixing length, our insertion) is small."

These findings, together with the finding discussed in section 3.5 suggest a further revision of the spin up cartoon shown in Fig. 1. The revised cartoon is shown in Fig. 7. The conventional mechanism of spin up applies to explain the spin up of the circulation outside the eyewall updraught. The eyewall updraught, itself, is spun up by the mean vertical advection of high tangential momentum from the boundary layer and by the resolved eddy momentum fluxes discussed above.

5 Potential intensity theory

Our understanding of hurricanes has been influenced strongly by the simple, axisymmetric, steady-state hurricane model described in a pioneering study by (Emanuel, 1986, henceforth E86). This model has served to underpin many ideas about how tropical cyclones function. It provided the foundation for the so-called 'potential intensity (PI) theory' of tropical cyclones (Emanuel 1988, 1995; Bister and Emanuel 1998) and its time-dependent extension led to the formulation of the WISHE paradigm for intensification (Emanuel 1989, 1997, 2003, 2012) referred to in section 3.

PI theory refers to a theory for the maximum possible intensity that a storm could achieve in a particular environment, based on the maximum possible tangential wind component (specifically the maximum *gradient wind*[11]). That such an upper bound on intensity should exist follows

[11] In the Emanuel (1988) formulation for the maximum intensity of hurricanes, intensity was characterized by the minimum surface pressure. In subsequent papers, the formulation for the minimum surface pressure was revised and focus was shifted to the maximum gradient wind.

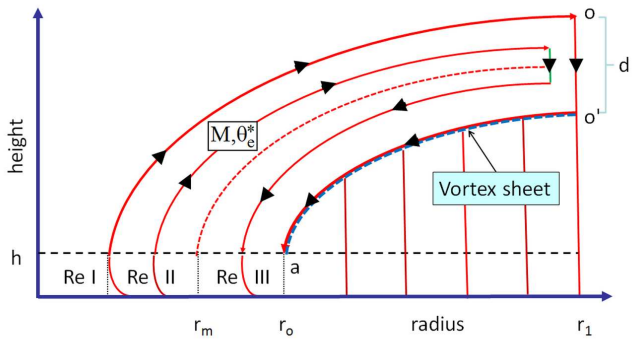

Figure 8. Schematic diagram of Emanuel's 1986 model for a steady-state mature hurricane. The arrows indicate the direction of the overturning circulation. See text for discussion.

from global energy considerations. Under normal circumstances, the energy dissipation associated with surface friction scales as the cube of the tangential winds, while the energy input via moist entropy fluxes scales generally with the first power of the wind[12]. It follows that the frictional dissipation will exceed the input of latent heat energy to the vortex from the underlying ocean at some point during the cyclone's intensification[13]. It is important to point out that most storms never reach their PI (Merrill 1988, Fig. 1; DeMaria and Kaplan 1994, Fig. 1; Emanuel 1999)[14].

Despite the uncertainties with the theory to be discussed below, PI theory has been used widely to estimate the impact of global climate change on tropical cyclone intensity and structure change. As an example of its far-reaching influences, the E86 theory is still used as a basis for deriving updates to the *a priori* PI theory (Bryan and Rotunno 2009a; Garner 2015) as well as for estimates of the impact of tropical cyclone intensity and structure change due to global warming scenarios (Emanuel 1988; Camargo et al. 2014).

[12]There is a subtle caveat with this scaling argument because the linear dependence of the energy input on wind speed may be suppressed if the degree of moisture disequilibrium at the sea surface is reduced as the wind speed increases.

[13]It is presently thought there is an exception to this argument when either the sea surface temperature is sufficiently warm or the upper tropospheric temperature is sufficiently cold, or some combination of the two prevails (Emanuel 1988). Under such extreme conditions, the vortex is believed to be capable of generating enough latent heat energy via surface moisture fluxes to more than offset the dissipation of energy and a 'runaway' hurricane - the so-called 'hypercane regime' - is predicted. Strictly speaking, however, these predictions have been formulated only in the context of axisymmetric theory and simulated using subsonic, axisymmetric flow codes. It remains an open question whether hypercanes are dynamically realizable in a realistic, three-dimensional flow configuration.

[14]Reasons why most storms do not reach their PI are attributed to the deleterious effects of vertical shear, that tends to tilt/deform a developing vortex and to open pathways for dry air intrusion (Riemer et al. 2010; Tang and Emanuel 2010; Riemer and Montgomery 2011).

5.1 Emanuel's steady-state model

Figure 8 shows a schematic of Emanuel's 1986 steady-state hurricane model. The energetics of this model are often likened to that of a Carnot cycle in which the inflowing air acquires heat (principally latent heat) while remaining approximately isothermal. The ascending air is assumed to be moist adiabatic and the outflowing air at large radius is assumed to descend isothermally in the upper atmosphere. The final leg in the cycle is assumed to follow a reversible moist adiabat. Recent work by Bister et al. (2010) has pointed out, *inter alia*, that this hypothetical dissipative heat engine does no useful work on its environment.

The E86 model assumes hydrostatic balance and gradient wind balance above the boundary layer and uses a quasi-linear slab boundary model in which departures from gradient wind balance are negligibly small. The boundary layer is assumed to have constant depth h in which M and pseudo-equivalent potential temperature θ_e are well mixed. This layer is divided into three regions as shown in Fig. 8: the eye (Re I), the eyewall (Re II) and outside the eyewall (Re III) where spiral rainbands and shallow convection are assumed to form in the vortex above. The quantities M and θ_e, are assumed to be materially conserved after the parcel leaves the boundary layer and ascends in the eyewall cloud[15].

In the steady model, the parcel trajectories are streamlines of the secondary circulation along which M and θ_e are materially conserved. The precise values of these quantities at a particular radius are determined by the frictional boundary layer. The model assumes that the radius of maximum tangential wind speed, r_m, is located at the outer edge of the eyewall cloud, although recent observations indicate it is closer to the inner edge (Marks et al. 2008). The middle dashed curve emanating from r_m is the M-surface along which the vertical velocity is zero and demarcates the region of ascent in the eyewall from that of large-scale descent outside the eyewall. The outer dashed curve indicates the location of the vortex sheet as described in Smith et al. (2014). The flow segment between o and o' in the upper right corner of the figure represents the assumed isothermal leg noted above and is the location at which air parcels are assumed to steadily gain cyclonic relative angular momentum (RAM, rv) from the environment. The gain of RAM is needed order to replace the frictional loss of angular momentum at the surface where the flow is cyclonic. This source of RAM is required for a steady state to exist and it is pertinent to enquire whether this source is physically plausible (see section 6).

Aside from the assumption of axial symmetry and realism of the source of RAM, the model suffers a range of issues as discussed by Smith et al.

[15]Contrary to statements made in E86, the formulation assumes pseudo-adiabatic rather than reversible thermodynamics in which all condensate instantaneously rains out (Bryan and Rotunno 2009a, p3044). It is not a true Carnot cycle, in part, because of the irreversible nature of the precipitation process in the eyewall region of the vortex.

(2008), Bryan and Rotunno (2009b), Emanuel (2012) and Montgomery and Smith (2014) (and summarized below).

The original formulation for the PI leads to an equation for V_{max}^2 (Eq. (43) in E86):

$$V_{max}^2 = \frac{C_\theta}{C_D}\epsilon L q_a^*(1-RH_{as})\frac{1-\frac{f^2 r_o^2}{4\beta R T_B}}{1-\frac{1}{2}\frac{C_\theta}{C_D}\epsilon\frac{L q_a^*(1-RH_{as})}{\beta R T_s}} \tag{18}$$

where V_{max} is the maximum gradient wind, L is the latent heat of condensation of water vapour, T_s is the sea surface temperature, C_θ is the surface exchange coefficient of moist entropy (and enthalpy), C_D is the drag coefficient, $\epsilon = (T_B - T_0)/T_B$ is the thermodynamic efficiency factor, T_B is the averaged temperature of the boundary layer (assumed constant with radius), T_0 is the average outflow temperature weighted with the saturated moist entropy of the outflow angular momentum surfaces (Eq. (19) of Emanuel 1986)[16], q_a^* is the saturation mixing ratio at the top of the surface layer in the environment, RH_{as} is the ambient relative humidity at the top of the surface layer, $\beta = 1 - \epsilon(1 + Lq_a^* RH_{as}/RT_s)$ and r_o is the radial extent of the storm near sea level (nominally the radius at which $V = 0$)[17].

From Eq. (18), Emanuel constructed curves for V_{max} as a function of upper-level outflow temperature and sea surface temperature. As an example, for a sea surface temperature of 28^oC and an outflow temperature of -60^o C, the formula predicts a V_{max} of approximately 58 m s^{-1} (see Fig. 9). In this calculation, it has been assumed that C_θ/C_D = 1, but the latest field observations and laboratory measurements synthesized in Bell et al. (2012) suggest a mean value of approximately $C_\theta/C_D = 0.5$ in the high wind speed range. Although Bell et al. (2012) acknowledge the scatter in the latest observational estimates of C_θ/C_D in the high wind speed regime, these data represent our best estimates. For this reduced ratio of exchange coefficients, Eq. (18) predicts a reduced V_{max} of approximately 42 m s^{-1}.

One puzzling feature of both the E86 derivation and its extensions discussed below is that there seems to be no constraint that $\partial v/\partial r = 0$ at the radius of maximum tangential wind. Moreover, all derivations within this formalism fail to predict the radius of maximum tangential wind (at least without introducing other unknown quantities)!

Some major hurricanes can significantly exceed the value predicted by Eq. (18). One such example is the case of Hurricane Isabel (2003) (Montgomery et al. 2006a and Bell and Montgomery 2008), which has been shown to exceed its predicted PI for three consecutive days. As an example, on 13 September, Isabel had an observed maximum tangential wind of approximately 76 m s^{-1}, yet a best estimate[18] based on Eq. (18) using in retrospect an arguably liberal $C_\theta/C_D = 1$ gives only 56.6 m s^{-1}. In this case, there is a discrepancy of approximately 20 m s^{-1} between the theory and the observations. The discrepancy spans at least two intensity categories on the Saffir-Simpson hurricane scale (Category 3 to Category 5). The fact that some major hurricanes in regions of the world oceans can significantly exceed this theoretical predicted intensity for sea surface temperatures of 28^o C (or higher) is presumably a consequence of certain assumptions made in formulating the E86 model.

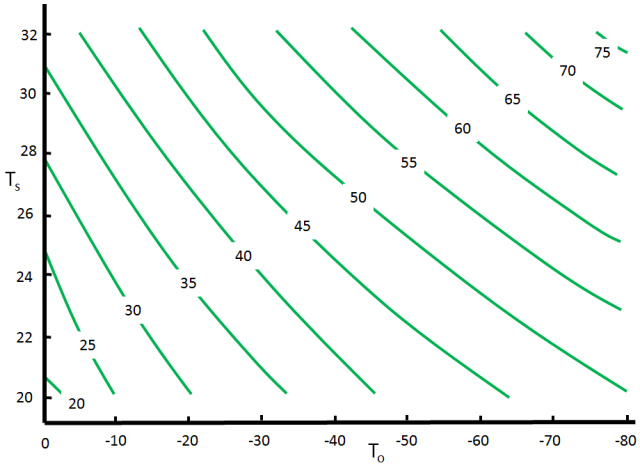

Figure 9. Predicted V_{max} from Eq. (18) as a function of sea surface temperature (T_s) and outflow temperature (T_o) from Emanuel's 1986 model for a mature steady-state hurricane. Temperature is in Celsius. The ratio of moist entropy to momentum transfer coefficients C_θ/C_D is assumed to be unity. Calculations assume an ambient surface pressure of 1015 mb, an ambient relative humidity (RH) of 80 %, a Coriolis parameter f evaluated at 20 degrees latitude, and an outer radius r_0 equal to 500 km. See text for further details. Adapted from Emanuel (1986).

High resolution axisymmetric numerical simulations have been conducted to test the original PI theory in a controlled setting (Persing and Montgomery 2003; Hausman et al. 2006; Bryan and Rotunno 2009a). For horizontal mixing lengths consistent with recently observed estimates from flight-level data in major hurricanes (Zhang and Montgomery 2012), the numerical studies of Persing and Montgomery (2003) and Bryan and Rotunno (2009a) confirm the tendency for solutions to significantly exceed the theoretically predicted PI given by Eq. (18) and its modifications summarized below.

5.2 Unbalanced effects

Important limitations of E86 theory are its neglect of unbalanced dynamics in the frictional boundary layer (Smith et al. 2008) and above the boundary layer (Bryan and Rotunno 2009b). Bryan and Rotunno derived

[16]This is the temperature at which air parcels are assumed to descend approximately isothermally in the upper atmosphere.

[17]The mathematical definition for r_0 is given by Eq. (20) of Emanuel 1986.

[18]This estimate takes into account the uncertainty of the exchange coefficients and the ocean cooling effect by turbulence-induced upwelling of cooler water from below the thermocline by assuming a ratio of exchange coefficients of unity and that dissipative heating offsets ocean cooling. See Montgomery et al. (2006a) and Bell and Montgomery (2008) for further details and footnote 19 for an update on the matter of dissipative heating.

a modified formula for V_{max} which accounts for unbalanced processes above the boundary layer. The formula is $V_{max}^2 = EPI^2 + \gamma$, where EPI is V_{max} as given by Eq. (18), $\gamma = \alpha r_{max} \eta_b w_b$ and these latter terms are evaluated at the top of the boundary layer at the location of maximum tangential velocity (which, as noted above, is not predicted by the theory, itself). Here, $\eta = \partial u/\partial z - \partial w/\partial r$ is the azimuthal component of vorticity, r_{max} is the radius of V_{max}, w_b is the vertical velocity at the top of the boundary layer at this same radius and $\alpha = T_s/T_o$, where T_s is the SST and T_o is the outflow temperature. The α term is associated with the inclusion of dissipative heating (the increase in internal energy associated with the dissipation of kinetic energy) in the PI formulation of Bister and Emanuel (1998)[19].

Bryan and Rotunno showed that

$$\eta_b w_b \approx \left(\frac{v^2}{r} - \frac{v_g^2}{r} \right), \qquad (19)$$

where v is the total tangential velocity and v_g is the tangential velocity in gradient wind balance with the radial pressure gradient force per unit mass, both of which are evaluated at the top of the boundary layer. They point out that, in a supergradient flow, the right-hand-side of this equation is positive, whereupon γ on the right-hand-side of Eq. (19) is a positive contribution to V_{max}. In the limiting case of small horizontal mixing length, they find that $\gamma \approx EPI$ so that (p3055) " ... the effects of unbalanced flow contribute as much to maximum intensity as balanced flow for this case". In the case of Hurricane Isabel, the new formula was a significant improvement and despite uncertainties in the observations, Bryan and Rotunno concluded that "... unbalanced flow effects are not negligible in some tropical cyclones and that they contribute significantly to maximum intensity".

Bryan and Rotunno's extended analytical theory is not an *a priori* form of PI in the sense of using only environmental conditions as input: it requires knowledge also of η_b, r_{max} and w_b. Thus one cannot make graphs of V_{max} as functions of SST and outflow temperature similar to Fig. 9. The theory continues to use the same boundary layer formulation as E86 (see their section 2b). In essence, the flow in the boundary layer is assumed to be in approximate gradient wind balance. For this reason, the new theory does not address the concerns raised about the original theory by Smith et al. (2008).

Clearly, a more complete boundary layer formulation that includes a radial momentum equation would be required to determine η_b, r_{max} and w_b, and thereby V_{max}. Indeed, it is these three quantities (η_b, r_{max} and w_b) that characterize the effect of 'boundary layer control' on the eyewall dynamics discussed by Kilroy et al. (2015) and Schmidt and Smith (2015) (see section 3.8). In this sense, Bryan and Rotunno's analysis provides further evidence that unbalanced effects in the boundary layer are responsible for those in the eyewall. When η_b, r_{max} and w_b are diagnosed from a numerical simulation (with an unbalanced boundary layer), the new formula for V_{max} is shown to provide an accurate estimate for the maximum intensity of numerically simulated vortices by Bryan and Rotunno (2009b) for a range of values of the horizontal mixing length (see Bryan and Rotunno 2009a, Fig. 12)[20].

The work of Bryan and Rotunno (2009a) and subsequent work by Rotunno and Bryan (2012) and Bryan (2013) have emphasized the strong dependence of the simulated intensity in *axisymmetric* models to the horizontal mixing length (and related diffusivity) used to parameterize asymmetric mixing and small-scale turbulence.

5.3 A revised theory

Emanuel and Rotunno (2011) and Emanuel (2012) pointed out that the assumption of the original model that the air parcels rising in the eyewall exit in the lower stratosphere in a region of approximately constant absolute temperature is questionable. In the second of these papers, Emanuel *op. cit.* stated that "... Emanuel and Rotunno (2011, hereafter Part I) demonstrated that in numerically simulated tropical cyclones, the assumption of constant outflow temperature is poor and that, in the simulations, the outflow temperature increases rapidly with angular momentum." To address these issues, a revised theory was proposed in which the absolute temperature stratification of the outflow is determined by small-scale turbulence that limits the gradient Richardson number to a critical value. Ordinarily, the Richardson number criterion demarcates the boundary between stratified shear stability and instability/turbulence. Here it seems that small-scale turbulence in the outflow layer is presumed to operate and limit the Richardson number to a critical value.

The new theory represents a major shift in the way that the storm is influenced by its environment. In the

[19] A recent theoretical study by Kieu (2015) has suggested an inconsistency of the Bister and Emanuel formulation and related assumption that all dissipative heating in the atmospheric surface layer can return to the atmosphere as an 'additional' heat source that acts to augment the maximum gradient wind of the vortex. Kieu (2015) recommends use of the original PI formation of Emanuel (1986), since (conclusions) "it can be reinterpreted as a rational estimation of the TC MPI (tropical cyclone maximum potential intensity - our insertion) even in the presence of the internal dissipative heating ..." Drawing upon the observational analyses of Zhang (2010), Kieu (2015) suggests that the dissipative heating formulation used by Bister and Emanuel (1998) and Bryan and Rotunno (2009a,b) overestimates the true dissipative heating in part due to an inaccurate estimate of the viscous work term in the boundary layer and also in part to the radiation of energy out of the hurricane by wind-induced surface gravity waves at the air-sea interface. This interesting topic would appear to merit further study.

[20] Notwithstanding the good agreement, there would appear to be two issues with the comparison of PI theory with their numerical calculation, both acknowledged in their paper. Firstly, the PI is calculated at the radius of V_{max} in the model rather than at the radius of maximum gradient wind of either the theory or the model. The second issue is the calculation of the gradient wind from the pressure field in the full model output, which incorporates substantial unbalanced effects as well as the balanced effects contained in the E86 model.

previous version, it was assumed that the thermal structure of the lower stratosphere determined the (constant) outflow temperature. In the revised theory, the vertical structure of the outflow temperature is set internally within the vortex and, in principal, no longer matches the temperature structure of the environment. This shift in the formulation would appear to have ramifications for the theory advanced by Nong and Emanuel (2003) as to how upper troughs interact with the vortex and excite the process of inner-core wind amplification.

The revised theory generally predicts a reduced intensity by a factor of $1/\sqrt{2}$ compared with the original formula given above (see Emanuel and Rotunno 2011, pp2246-2247). However, it is difficult to assess the precise change in V_{max} between the two theories for the case of Hurricane Isabel or other observed storms because, in the new theory, the effects of dissipative heating and the increase of the saturation specific humidity with decreasing pressure are excluded. In axisymmetric numerical model simulations used to test the new theory, Emanuel and Rotunno used also large values of vertical mixing length to " ... prevent the boundary flow from becoming appreciably supergradient" (see their p994), thereby keeping the tests consistent with a key assumption of the theory. Emanuel and Rotunno (2011) argued that because the axisymmetric numerical model includes the foregoing effects and provides good agreement with the theory, these effects must approximately cancel. This cancellation would imply that the revised theory is not an improvement to explain the discrepancy between the theory and observations in Isabel as discussed above.

5.4 Three dimensional effects

There are significant differences in behaviour between tropical cyclone simulations in axisymmetric and three-dimensional models (Yang et al. 2007; Bryan et al. 2009; Persing et al. 2013). These studies have shown that three-dimensional models predict a significantly reduced intensity (15-20%) compared to their axisymmetric counterparts. In particular, in three-dimensional model simulations with parameter settings that are consistent with recent observations of turbulence in hurricanes, Persing et al. (2013) showed little support for the upper troposphere mixing hypothesis of Emanuel and Rotunno (2011). In their three-dimensional simulations, Persing et al. (2013) found that values of the gradient Richardson number were generally far from criticality with correspondingly little turbulent mixing in the upper level outflow region within approximately 100 km from the storm centre: only marginal criticality was suggested during the mature stage. Based on these findings, it seems clear that three-dimensional effects should be accounted for properly in a consistent formulation of the maximum intensity problem.

Bryan and Rotunno (2009b) pointed out that some of their own reported results "might be specific to axisymmetric models and should someday be re-evaluated using three-dimensional simulations". This remark would seem to apply not only to their results.

6 Revisiting steady-state tropical cyclones

A recent study by Smith et al. (2014) has questioned the existence of a realistic globally-steady-state tropical cyclone. By global steady state we mean that the macroscale flow does not vary systematically with time. Among other things, echoing Anthes (1972), the Smith et al. study showed that if such a state were to exist, then a source of cyclonic RAM would be necessary to maintain the vortex against the frictional loss of angular momentum at the sea surface. It showed also that while a supply of cyclonic RAM is a necessary condition for a globally steady state cyclone, it is not sufficient. The vanishing of the spin up function above the boundary layer and outside regions where turbulent diffusion is significant would be necessary also. It would seem to be a logical consequence that, without a steady source of cyclonic RAM, tropical cyclones must be globally transient, a deduction that accords with observations. For example, in the E86 model, cyclonic RAM is assumed to be steadily replenished at large radii in the upper troposphere.

In more general cases, which attain a quasi-steady state, a natural question arises as to the source of RAM needed to support this state. Chavas and Emanuel (2014) presented solutions for long-time sustained hurricanes using the Bryan cloud model in an axisymmetric configuration. Although they noted the limitations of their findings because of the long-time required to achieve the equilibrium regime and the unlikelihood of observing quasi-steady hurricanes in reality over a several day period, they did consider the primary source of RAM in one of their solutions. Using a surface torque balance for their control experiment, they reported that their sustained hurricane simulation managed to maintain itself indefinitely via the replenishment of RAM by vertical diffusion at the surface in the anticyclonic portion of the outer vortex, as predicted by Smith et al. (2014).

Solutions for one or more sustained hurricanes lasting for 20 or more days have been found to exist in three-dimensional doubly-periodic rectangular domains (Khairoutdinov and Emanuel 2013; Zhuo et al. 2014). While these solutions appear to be plausible sustained hurricanes, it is nonetheless true that the theoretical considerations of Smith et al. (2014) should still provide a means of identifying where the source of cyclonic RAM must originate for each individual hurricane to maintain itself. However, the needed source of cyclonic RAM was not investigated by these latter authors and the precise sources of RAM in these solutions remains unknown.

7 Conclusions

We have reviewed progress in understanding the fluid dynamics and moist thermodynamics of tropical cyclone vortices spanning the last two and a half decades since the first review in this journal. Because of space limitations and the tremendous growth in the science of the subject,

we have had to limit the review to the dynamics and moist thermodynamics of vortex intensification and structure and the role of coherent eddy structures in the evolution of these vortices. Important topics, such as the formation of these vortices, their movement, their interaction with larger-scale weather systems, their extratropical transition, as well as the formation of vortex sub-structures such as vortex Rossby waves, eyewall mesovortices, or secondary (outer) eyewalls have not been covered.

Beginning with a brief summary of the basic equations and a short review of moist thermodynamics and key aspects of moist deep cumulus convection, elementary consequences of rotation and local buoyancy in rotating flows were discussed. Previous paradigms for intensification were reviewed briefly, but the main emphasis is on a new rotating convection paradigm in which cloud buoyancy and vortex-tube-stretching are key elements. The frictional boundary layer plays a crucial role in the convective organization and system-scale dynamics of the spin up process. This boundary layer has been found to exert also a strong control on the location of the eyewall updraught, and the thermal properties of the updraught. A newly recognized feature of the spin up process is that a sloping eyewall is spun up by the vertical advection of high tangential momentum from the boundary layer and not by the conventional mechanism of spin up, i.e. through the radial import of absolute vorticity. Another newly recognized feature of the spin up process is through the radial and vertical divergence of eddy momentum fluxes, the latter of which is identified with the azimuthally-averaged non-advective vorticity flux. During spin up, these fluxes are typically counter-gradient and have no counterpart in strictly axisymmetric descriptions of these vortices.

We have reviewed the pioneering work describing mature hurricanes as axisymmetric, dissipative heat engines, which led to a theory for the maximum potential intensity of these storms. In particular, we have appraised recent modifications of the original theory and have pointed to a number of limitations of the theory. Finally, we have reviewed other recent work calling into question the existence of a globally quasi-steady tropical cyclone.

Acknowledgement

MTM acknowledges the support of NSF AGS-1313948, NOAA HFIP grant N0017315WR00048, NASA grant NNG11PK021 and the U.S. Naval Postgraduate School. RKS acknowledges financial support from the German Research Council (Grant SM30-23) and the Office of Naval Research Global (Grant N62909-15-1-N021). We thank J. Persing and G. Kilroy for their valuable comments on a near-final draft of the manuscript. The views expressed herein are those of the authors and do not represent sponsoring agencies or institutions.

References

Abarca, S. F. and M. T. Montgomery, 2013: Essential dynamics of secondary eyewall formation. *J. Atmos. Sci.*, **70**, 3216–3420.

Abarca, S. F., M. T. Montgomery, and J. C. McWilliams, 2015: The azimuthally-averaged boundary layer structure of a numerically simulated major hurricane. *J. Adv. Model. Earth Syst.*, **07**, 10.1002/.

Anthes, R. A., 1972: Development of asymmetries in a three-dimensional numerical model of the tropical cyclone. *Mon. Wea. Rev.*, **100**, 461–476.

Batchelor, G. K., 1967: *An introduction to fluid dynamics*. Cambridge University Press, Cambridge, England, 615pp.

Bell, M. M. and M. T. Montgomery, 2008: Observed structure, evolution, and potential intensity of category 5 Hurricane Isabel (2003) from 12 to 14 september. *Mon. Wea. Rev.*, **136**, 2023–2046.

Bell, M. M. and M. T. Montgomery, 2010: Sheared deep vortical convection in pre-depression Hagupit during TCS08. *Geo. Res. Letters*, **37**, l06802.

Bell, M. M., M. T. Montgomery, and K. A. Emanuel, 2012: Air-sea enthalpy and momentum exchange atmajor hurricane wind speeds observed during CBLAST. *J. Atmos. Sci.*, **69**, 3197–3222.

Bister, M. and K. A. Emanuel, 1998: Dissipative heating and hurricane intensity. *Meteor. Atmos. Phys.*, **50**, 233–240.

Bister, M., N. Renno, O. Paulius, and K. A. Emanuel, 2010: Comment on makarieva et al. a critique of some modern applications of the carnot heat engine concept: the dissipative heat engine cannot exist. *Proc. R. Soc. A*, 1–6, doi:10.1098/rspa.2010.0087.

Braun, S. A., M. T. Montgomery, K. J. Mallen, and P. D. Reasor, 2010: Simulation and interpretation of the genesis of Tropical Storm Gert (2005) as part of the NASA Tropical Cloud Systems and Processes Experiment. *J. Atmos. Sci.*, **67**, 999–1025.

Bryan, G. H., 2013: Notes and correspondence comments on “sensitivity of tropical-cyclone models to the surface drag coefficient”. *Quart. Journ. Roy. Meteor. Soc.*, **139**, 1957–1960.

Bryan, G. H. and R. Rotunno, 2009a: Evaluation of an analytical model for the maximum intensity of tropical cyclones. *J. Atmos. Sci.*, **66**, 3042–3060.

Bryan, G. H. and R. Rotunno, 2009b: The maximum intensity of tropical cyclones in axisymmetric numerical model simulations. *Mon. Wea. Rev.*, **137**, 1770–1789.

Bryan, G. H., R. Rotunno, and Y. Chen, 2009: The effects of turbulence on hurricane intensity. *29th Conference on Hurricanes and Tropical Meteorology*, **66**, 3042–3060.

Camargo, S. J., M. K. Tippett, A. H. Sobel, G. A. Vecchi, and M. Zhao, 2014: Testing the performance of tropical cyclone genesis indices in future climates using the HIRAM model. *J. Climate*, **27**, 9171–9196.

Chan, J. C. L., 2005: The physics of tropical cyclone motion. *Annu. Rev. Fluid Mech.*, **37**, 99–128.

Chan, K. T. F. and J. C. L. Chan, 2014: Impacts of vortex intensity and outer winds on tropical cyclone size. *Quart. Journ. Roy. Meteor. Soc.*, **141**, 525–537.

Chavas, D. R. and K. Emanuel, 2014: Equilibrium tropical cyclone size in an idealized state of axisymmetric radiative convective equilibrium. *J. Atmos. Sci.*, **71**, 1663–1680.

Chen, Y., G. Brunet, and M. K. Yau, 2003: Spiral bands in a simulated hurricane. Part II: Wave activity diagnosis. *J. Atmos. Sci.*, **60**, 1239–1256.

DeMaria, M. and J. Kaplan, 1994: Sea surface temperature and the maximum intensity of Atlantic tropical cyclones. *J. Climate*, **7**, 1324–1334.

DeMaria, M., M. Mainelli, L. K. Shay, J. A. Knaffand, and J. Kaplan, 2005: Further improvements to the Statistical Hurricane Intensity Prediction Scheme (SHIPS). *Wea. Forecasting*, **20**, 531–543.

DeMaria, M. and J. D. Pickle, 1988: A simplified system of equations for simulation of tropical cyclones. *J. Atmos. Sci.*, **45**, 1542–1554.

Dritschel, D. G. and D. Waugh, 1992: Quantification of the inelastic interaction of unequal vortices in two-dimensional vortex dynamics. *Phys. Fluids*, **4**, 1737–1744.

Emanuel, K. A., 1986: An air-sea interaction theory for tropical cyclones. Part I: Steady state maintenance. *J. Atmos. Sci.*, **43**, 585–604.

Emanuel, K. A., 1988: The maximum intensity of hurricanes. *J. Atmos. Sci.*, **45**, 1143–1155.

Emanuel, K. A., 1989: The finite amplitude nature of tropical cyclogenesis. *J. Atmos. Sci.*, **46**, 3431–3456.

Emanuel, K. A., 1991: The theory of hurricanes. *Annu. Rev. Fluid Mech.*, **23**, 179–196.

Emanuel, K. A., 1994: *Atmospheric convection*. Oxford University Press. pp580.

Emanuel, K. A., 1995: Sensitivity of tropical cyclone to surface exchange coefficients and a revised steady-state model incorporating eye dynamics. *J. Atmos. Sci.*, **52**, 3969–3976.

Emanuel, K. A., 1997: Some aspects of hurricane inner-core dynamics and energetics. *J. Atmos. Sci.*, **54**, 1014–1026.

Emanuel, K. A., 1999: Thermodynamic control of hurricane intensity. *Nature*, **401**, 665–669.

Emanuel, K. A., 2003: Tropical cyclones. *Annu. Rev. Earth Planet. Sci.*, **31**, 75–104.

Emanuel, K. A., 2012: Self-stratification of tropical cyclone outflow. Part II: Implications for storm intensification. *J. Atmos. Sci.*, **69**, 988–996.

Emanuel, K. A., J. D. Neelin, and C. S. Bretherton, 1994: On large-scale circulations of convecting atmospheres. *Quart. Journ. Roy. Meteor. Soc.*, **120**, 1111–1143.

Emanuel, K. A. and R. Rotunno, 2011: Self-stratification of tropical cyclone outflow. Part I: Implications for storm structure. *J. Atmos. Sci.*, **68**, 2236–2249.

Fang, J. and F. Zhang, 2011: Evolution of multiscale vortices in the development of Hurricane Dolly (2008). *J. Atmos. Sci.*, **68**, 103–122.

Franklin, J. L., S. J. Lord, S. E. Feuer, and F. D. M. Jr., 1993: The kinematic structure of Hurricane Gloria (1985) determined from nested analyses of dropwindsonde and Doppler radar data. *Mon. Wea. Rev.*, **121**, 2433–2451.

Frisius, T., 2015: What controls the size of a tropical cyclone? Investigations with an axisymmetric model. *Quart. Journ. Roy. Meteor. Soc.*, **141**, 2457–2470.

Fudeyasu, H. and Y. Wang, 2011: Balanced contribution to the intensification of a tropical cyclone simulated in TCM4: Outer-core spinup process. *J. Atmos. Sci.*, **68**, 430–449.

Gall, R., J. Franklin, F. Marks, E. N. Rappaport, and F. Toepfer, 2013: The Hurricane Forecast Improvement Project. *Bull. Amer. Meteor. Soc.*, **94**, 329–343.

Garner, S., 2015: The relationship between hurricane potential intensity and CAPE. *J. Atmos. Sci.*, **72**, 141–163.

Gill, A. E., 1982: *Atmosphere - Ocean Dynamics*. Fourth Edition. Academic Press, Academic Press, New York, pp662.

Gopalakrishnan, S. G., F. Marks, X. Zhang, J. W. Bao, K. S. Yeh, and R. Atlas, 2011: The experimental HWRF system: A study on the influence of horizontal resolution on the structure and intensity changes in tropical cyclones using an idealized framework. *Mon. Wea. Rev.*, **139**, 1762–1784.

Greenspan, H. P. and L. N. Howard, 1963: On a time-dependent motion of a rotating fluid. *J. Fluid Mech.*, **17**, 385–404.

Hack, J. J. and W. H. Schubert, 1986: Nonlinear response of atmospheric vortices to heating by organized cumulus convection. *J. Atmos. Sci.*, **43**, 1559–1573.

Hakim, G. J., 2011: The mean state of axisymmetric hurricanes in statistical equilibrium. *J. Atmos. Sci.*, **68**, 1364–1376.

Hausman, S. A., K. V. Ooyama, and W. H. Schubert, 2006: Potential vorticity structure of simulated hurricanes. *J. Atmos. Sci.*, **63**, 87–108.

Hawkins, H. F. and S. M. Imbembo, 1976: The structure of a small, intense hurricane Inez 1966. *Mon. Wea. Rev.*, **104**, 418–442.

Hawkins, H. F. and D. T. Rubsam, 1968: Hurricane Hilda, 1964. *Mon. Wea. Rev.*, **96**, 617–636.

Haynes, P. and M. E. McIntyre, 1987: On the evolution of vorticity and potential vorticity in the presence of diabatic heating and frictional or other forces. *J. Atmos. Sci.*, **44**, 828–841.

Hendricks, E. A., M. T. Montgomery, and C. A. Davis, 2004: On the role of "vortical" hot towers in the formation of tropical cyclone Diana (1984). *J. Atmos. Sci.*, **61**, 1209–1232.

Heymsfield, G. M., J. B. Halverson, J. Simpson, L. Tian, and T. P. Bui, 2001: ER-2 Doppler radar investigations of the eyewall of Hurricane Bonnie during the convection and moisture experiment-3. *J. Appl. Met.*, **40**, 1310–1330.

Holton, J. R., 2004: *An introduction to dynamic meteorology, 4th Edition*. Academic Press, London, 535pp.

Houze, R. A., 2014: *Clouds dynamics, 2nd Edition*. Academic Press, London, 496pp.

Jones, C. W. and E. J. Watson, 1963: *Laminar boundary layers*, L. Rosenhead, Ed., Oxford University Press, pp687, 198–257.

Julien, K., S. Legg, J. C. McWilliams, and J. Werne, 1996: Rapidly rotating turbulent Rayleigh-Bénard convection. *J. Fluid Mech.*, **322**, 243–273.

Kepert, J. D., 2006a: Observed boundary-layer wind structure and balance in the hurricane core. Part I. Hurricane Georges. *J. Atmos. Sci.*, **63**, 2169–2193.

Kepert, J. D., 2006b: Observed boundary-layer wind structure and balance in the hurricane core. Part II. Hurricane Mitch. *J. Atmos. Sci.*, **63**, 2194–2211.

Kepert, J. D., J. Schwendike, and H. Ramsay, 2016: Why is the tropical cyclone boundary layer not "well mixed"? *J. Atmos. Sci.*, **73**, 957–973.

Khairoutdinov, M. and K. Emanuel, 2013: Rotating radiative-convective equilibrium simulated by a cloud-resolving model. *J. Adv. Model. Earth Syst.*, **05**, doi: 10.1002/2013MS000253.

Kieu, C., 2015: Revisiting dissipative heating in tropical cyclone maximum potential intensity. *Quart. Journ. Roy. Meteor. Soc.*, **139**, 1255–1269, doi:10.1002/qj.2534.

Kilroy, G. and R. K. Smith, 2013: A numerical study of rotating convection during tropical cyclogenesis. *Quart. Journ. Roy. Meteor. Soc.*, **139**, 1255–1269.

Kilroy, G. and R. K. Smith, 2015: Tropical-cyclone convection: the effects of a vortex boundary layer wind profile on deep convection. *Quart. Journ. Roy. Meteor. Soc.*, **141**, 714–726.

Kilroy, G., R. K. Smith, and M. T. Montgomery, 2015: Why do model tropical cyclones grow progressively in size and decay in intensity after reaching maturity? *J. Atmos. Sci.*, **72**, in press.

Klemp, J. B., 1987: Dynamics of tornadic thunderstorms. *Annu. Rev. Fluid Mech.*, **19**, 369–402.

Lansky, I. M., T. M. O'Meil, and D. A. Schecter, 1984: A theory of vortex merger. *Phys. Rev. Lett.*, **79**, 1479 –1482.

Li, T., X. Ge, M. Peng, and W. Wang, 2012: Dependence of tropical cyclone intensification on the Coriolis parameter. *Trop. Cycl. Res. Rev.*, **1**, 242–253.

Lussier, L. L., B. Rutherford, M. T. Montgomery, M. A. Boothe, and T. J. Dunkerton, 2015: Examining the roles of the easterly wave critical layer and vorticity accretion during the tropical cyclogenesis of Hurricane Sandy. *Mon. Wea. Rev.*, **143**, 1703–1722.

Marks, F. D., P. G. Black, M. T. Montgomery, and R. W. Burpee, 2008: Structure of the eye and eyewall of Hurricane Hugo (1989). *Mon. Wea. Rev.*, **136**, 1237–1259.

Melander, M. V., N. J. Zabusky, and J. C. McWilliams, 1988: Symmetric vortex merger in two dimensions: Causes and conditions. *J. Fluid Mech.*, **195**, 303–340.

Merrill, R. T., 1988: Environmental influences on hurricane intensification. *J. Atmos. Sci.*, **45**, 1678–1687.

Moeng, C. H., J. C. McWilliams, R. Rotunno, P. P. Sullivan, and J. Weil, 2004: Investigating 2D modeling of atmospheric convection in the PBL. *J. Atmos. Sci.*, **61**, 889–903.

Montgomery, M. T., M. M. Bell, S. D. Aberson, and M. L. Black, 2006a: Hurricane isabel (2003): New insights into the physics of intense storms. Part I mean vortex structure and maximum intensity estimates. *Bull Amer. Meteor. Soc.*, **87**, 1335–1348.

Montgomery, M. T. and J. Enagonio, 1998: Tropical cyclogenesis via convectively forced vortex Rossby waves in a three-dimensional quasigeostrophic model. *J. Atmos. Sci.*, **55**, 3176–3207.

Montgomery, M. T., S. V. Nguyen, R. K. Smith, and J. Persing, 2009: Do tropical cyclones intensify by WISHE? *Quart. Journ. Roy. Meteor. Soc.*, **135**, 1697–1714.

Montgomery, M. T., M. E. Nichols, T. A. Cram, and A. B. Saunders, 2006b: A vortical hot tower route to tropical cyclogenesis. *J. Atmos. Sci.*, **63**, 355–386.

Montgomery, M. T., J. Persing, and R. K. Smith, 2015: Putting to rest WISHE-ful misconceptions. *J. Adv. Model. Earth Syst.*, **07**, doi:10.1002/.

Montgomery, M. T. and R. K. Smith, 2014: Paradigms for tropical cyclone intensification. *Aust. Met. Ocean. Soc. Journl.*, **64**, 37–66.

Montgomery, M. T., J. A. Zhang, and R. K. Smith, 2014: An analysis of the observed low-level structure of rapidly intensifying and mature Hurricane Earl (2010). *Quart. Journ. Roy. Meteor. Soc.*, **140**, 2132–2146, doi:10.1002/qj.2283.

Nguyen, C. M., R. K. Smith, H. Zhu, and W. Ulrich, 2002: A minimal axisymmetric hurricane model. *Quart. Journ. Roy. Meteor. Soc.*, **128**, 2641–2661.

Nguyen, V. S., R. K. Smith, and M. T. Montgomery, 2008: Tropical-cyclone intensification and predictability in three dimensions. *Quart. Journ. Roy. Meteor. Soc.*, **134**, 563–582.

Nong, S. and K. A. Emanuel, 2003: A numerical study of the genesis of concentric eyewalls in hurricanes. *Quart. Journ. Roy. Meteor. Soc.*, **129**, 3323–3338.

Ooyama, K. V., 1969: Numerical simulation of the life cycle of tropical cyclones. *J. Atmos. Sci.*, **26**, 3–40.

Ooyama, K. V., 1982: Conceptual evolution of the theory and modeling of the tropical cyclone. *J. Meteor. Soc. Japan*, **60**, 369–380.

Persing, J. and M. T. Montgomery, 2003: Hurricane superintensity. *J. Atmos. Sci.*, **60**, 2349–2371.

Persing, J., M. T. Montgomery, J. McWilliams, and R. K. Smith, 2013: Asymmetric and axisymmetric dynamics of tropical cyclones. *Atmos. Chem. Phys.*, **13**, 12 299–12 341.

Rappin, E. D., M. C. Morgan, and G. J. Tripoli, 2011: The impact of outflow environment on tropical cyclone intensification and structure. *J. Atmos. Sci.*, **68**, 177–194.

Raymond, D. J. and C. L. Carillo, 2011: The vorticity budget of developing Typhoon Nuri (2008). *Atmos. Chem. Phys.*, **11**, 147–163.

Raymond, D. J., S. Gjorgjievska, S. L. Sessions, and Z. Fuchs, 2014: Tropical cyclogenesis and mid-level vorticity. *Aust. Met. Ocean. Soc. Journl.*, **64**, 11–25.

Reasor, P. D. and M. T. Montgomery, 2015: Evaluation of a heuristic model for tropical cyclone resilience. *J. Atmos. Sci.*, **72**, 1765–1782.

Reasor, P. D., M. T. Montgomery, and L. F. Bosart, 2005: Mesoscale observations of the genesis of Hurricane Dolly (1996). *J. Atmos. Sci.*, **62**, 3151–3171.

Riemer, M. and M. T. Montgomery, 2011: Simple kinematic models for the environmental interaction of tropical cyclones in vertical wind shear. *Atmos. Chem. Phys.*, **11**, 9395–9414.

Riemer, M., M. T. Montgomery, and M. E. Nicholls, 2010: A new paradigm for intensity modification of tropical cyclones: Thermodynamic impact of vertical wind shear on the inflow layer. *Atmos. Chem. Phys.*, **10**, 3163–3188.

Rogers, R. F. and Coauthors, 2006: The Intensity Forecasting Experiment: A NOAA multiyear field program for improving tropical cyclone intensity forecasts. *Bull. Amer. Meteor. Soc.*, **87**, 1523–1537.

Rogers, R. F., P. D. Reasor, and J. A. Zhang, 2015: Multiscale structure and evolution of Hurricane Earl (2010) during rapid intensification. *Mon. Wea. Rev.*, **143**, 536–562.

Rotunno, R., 2013: The fluid dynamics of tornadoes. *Ann. Rev. of Fluid Mech.*, **45**, 59–84, doi:10.1146/annurev-fluid-011212-140639.

Rotunno, R., 2014: Secondary circulations in rotating-flow boundary layers. *Aust. Met. Ocean. Soc. Journl.*, **64**, 27–35.

Rotunno, R. and G. H. Bryan, 2012: Effects of parameterized diffusion on simulated hurricanes. *J. Atmos. Sci.*, **69**, 2284–2299.

Rotunno, R. and K. A. Emanuel, 1987: An air-sea interaction theory for tropical cyclones. Part II Evolutionary study using a nonhydrostatic axisymmetric numerical model. *J. Atmos. Sci.*, **44**, 542–561.

Rozoff, C. M., D. S. Nolan, J. P. Kossin, F. Zhang, and J. Fang, 2012: The roles of an expanding wind field and inertial stability in tropical cyclone secondary eyewall formation. *J. Atmos. Sci.*, **69**, 2621–2643.

Sanger, N. T., M. T. Montgomery, R. K. Smith, and M. M. Bell, 2014: An observational study of tropical-cyclone spin-up in supertyphoon Jangmi from 24 to 27 September. *Mon. Wea. Rev.*, **142**, 3–28.

Schecter, D. A., 2011: Evaluation of a reduced model for investigating hurricane formation from turbulence. *Quart. Journ. Roy. Meteor. Soc.*, **137**, 155–178.

Schlichting, H., 1968: *Boundary Layer Theory, seventh Edition*. McGraw-Hill, New York, 817pp.

Schmidt, C. and R. K. Smith, 2015: Tropical cyclone evolution in a minimal axisymmetric model revisited. *Quart. Journ. Roy. Meteor. Soc.*, **140**, in press.

Schubert, W. H. and J. J. Hack, 1982: Inertial stability and tropical cyclone development. *J. Atmos. Sci.*, **39**, 1687–1697.

Shapiro, L. J. and M. T. Montgomery, 1993: A three-dimensional balance theory for rapidly-rotating vortices. *J. Atmos. Sci.*, **50**, 3322–3335.

Shin, S. and R. K. Smith, 2014: Tropical-cyclone intensification and predictability in a minimal three dimensional model. *Quart. Journ. Roy. Meteor. Soc.*, **134**, 1661–1671.

Sippel, J. A., J. W. Nielsen-Gammon, and S. Allen, 2006: The multiple vortex nature of tropical cyclogenesis. *Mon. Wea. Rev.*, **134**, 1796–1814.

Smith, R. K., 2003: A simple model of the hurricane boundary layer revisited. *Quart. Journ. Roy. Meteor. Soc.*, **129**, 1007–1027.

Smith, R. K., 2006: Accurate determination of a balanced axisymmetric vortex. *Tellus A*, **58**, 98–103.

Smith, R. K., 2007: Accurate determination of a balanced axisymmetric vortex: corrigendum and addendum. *Tellus A*, **59**, 785–786.

Smith, R. K., G. Kilroy, and M. T. Montgomery, 2015: Why do model tropical cyclones intensify more rapidly at low latitudes? *J. Atmos. Sci.*, **72**, 1783–1804.

Smith, R. K. and M. T. Montgomery, 2010: Hurricane boundary-layer theory. *Quart. Journ. Roy. Meteor. Soc.*, **136**, 1665–1670.

Smith, R. K. and M. T. Montgomery, 2015: The efficiency of diabatic heating and tropical cyclone intensification. *Quart. Journ. Roy. Meteor. Soc.*, **141**, in press.

Smith, R. K., M. T. Montgomery, and S. V. Nguyen, 2009: Tropical cyclone spin up revisited. *Quart. Journ. Roy. Meteor. Soc.*, **135**, 1321–1335.

Smith, R. K., M. T. Montgomery, and J. Persing, 2014: On steady-state tropical cyclones. *Quart. Journ. Roy. Meteor. Soc.*, **140**, 2638–2649, doi:10.1002/qj.2329.

Smith, R. K., M. T. Montgomery, and S. Vogl, 2008: A critique of Emanuel's hurricane model and potential intensity theory. *Quart. Journ. Roy. Meteor. Soc.*, **134**, 551–561.

Smith, R. K., M. T. Montgomery, and H. Zhu, 2005: Buoyancy in tropical cyclones and other rapidly rotating vortices. *Dyn. Atmos. Oceans*, **40**, 189–208.

Smith, R. K., C. W. Schmidt, and M. T. Montgomery, 2011: Dynamical constraints on the intensity and size of tropical cyclones. *Quart. Journ. Roy. Meteor. Soc.*, **137**, 1841–1855.

Smith, R. K. and G. L. Thomsen, 2010: Dependence of tropical-cyclone intensification on the boundary layer representation in a numerical model. *Quart. Journ. Roy. Meteor. Soc.*, **136**, 1671–1685.

Smith, R. K. and S. Vogl, 2008: A simple model of the hurricane boundary layer revisited. *Quart. Journ. Roy. Meteor. Soc.*, **134**, 337–351.

Tang, B. and K. A. Emanuel, 2010: Midlevel ventilations constraint on tropical cyclone intensity. *J. Atmos. Sci.*, **67**, 1817–1830.

Tory, K. J., M. T. Montgomery, and N. E. Davidson, 2006: Prediction and diagnosis of tropical cyclone formation in an NWP system. Part I: The critical role of vortex enhancement in deep convection. *J. Atmos. Sci.*, **63**, 3077–3090.

Vigh, J. L. and W. H. Schubert, 2009: Rapid development of the tropical cyclone warm core. *J. Atmos. Sci.*, **66**, 3335–3350.

Wissmeier, U. and R. K. Smith, 2011: Tropical-cyclone convection: the effects of ambient vertical vorticity. *Quart. Journ. Roy. Meteor. Soc.*, **137**, 845–857.

Xu, J. and Y. Wang, 2010: Sensitivity of tropical cyclone inner-core size and intensity to the radial distribution of surface entropy flux. *J. Atmos. Sci.*, **67**, 1831–1852.

Yamasaki, M., 1968: Numerical simulation of tropical cyclone development with the use of primitive equations. *J. Meteor. Soc. Japan*, **46**, 178–201.

Yang, B., Y. Wang, and B. Wang, 2007: The effect of internally generated inner-core asymmetrics on tropical cyclone potential intensity. *J. Atmos. Sci.*, **64**, 1165–1188.

Zhang, D.-L., Y. Liu, and M. K. Yau, 2001: A multi-scale numerical study of Hurricane Andrew (1992). Part IV: Unbalanced flows. *Mon. Wea. Rev.*, **61**, 92–107.

Zhang, J. A., 2010: Estimation of dissipative heating using low-level in situ aircraft observations in the hurricane boundary layer. *J. Atmos. Sci.*, **67**, 1853–1862.

Zhang, J. A. and F. D. Marks, 2015: Effects of horizontal diffusion on tropical cyclone intensity change and structure in idealized three-dimensional numerical simulations. *Mon. Wea. Rev.*, **143**, 92–107, doi:10.1175/MWR-D-14-00341.1.

Zhang, J. A. and M. T. Montgomery, 2012: Observational estimates of the horizontal eddy diffusivity and mixing length in the low-level region of intense hurricanes. *J. Atmos. Sci.*, **69**, 1306–1316.

Zhang, J. A., R. F. Rogers, D. S. Nolan, and F. D. Marks, 2011: On the characteristic height scales of the hurricane boundary layer. *Mon. Wea. Rev.*, **139**, 2523–2535.

Zhuo, W., I. M. Held, and S. T. Garner, 2014: Parameter study of tropical cyclones in rotating radiative-convective equilibrium with column physics and resolution of a 25-km GCM. *J. Atmos. Sci.*, **71**, 1058–1069.